Spectroscopy from Space

Roger N. Clark, Gregg A Swayze

U. S. Geological Survey
MS964, Box 25046 Federal Center
Denver, Colorado 80225, U.S.A.

rclark@usgs.gov
gswayze@usgs.gov

Robert Carlson

Jet Propulsion Laboratory, 183-601
California Institute of Technology
Pasadena, California 91109, U.S.A.

Robert.W.Carlson@jpl.nasa.gov

Will Grundy

Lowell Observatory
1400 West Mars Hill Road
Flagstaff, Arizona 86001, U.S.A.

W.Grundy@lowell.edu

Keith Noll

NASA/GSFC
MS 693
Greenbelt, Maryland 20771, U.S.A.

keith.s.noll@nasa.gov

ABSTRACT

This chapter reviews detection of materials on solid and liquid (lakes and ocean) surfaces in the solar system using ultraviolet to infrared spectroscopy from space, or near space (high altitude aircraft on the Earth), or in the case of remote objects, earth-based and earth-orbiting telescopes. Point spectrometers and imaging spectrometers have been probing the surfaces of our solar system for decades. Spacecraft carrying imaging spectrometers are currently in orbit around Mercury, Venus, Earth, Mars, and Saturn, and systems have recently visited Jupiter, comets, asteroids, and one spectrometer-carrying spacecraft is on its way to Pluto. Together these systems are providing a wealth of data that will enable a better understanding of the composition of condensed matter bodies in the solar system.

Minerals, ices, liquids, and other materials have been detected and mapped on the Earth and all planets and/or their satellites where the surface can be observed from space, with the exception of Venus whose thick atmosphere limits surface observation. Basaltic minerals (e.g., pyroxene and olivine) have been detected with spectroscopy on the Earth, Moon, Mars and some asteroids. The greatest mineralogic diversity seen from space is observed on the Earth and Mars. The Earth, with oceans, active tectonic and hydrologic cycles, and biological processes, displays the greatest material diversity including the detection of amorphous and crystalline inorganic materials, organic compounds, water and water ice.

Water ice is a very common mineral throughout the Solar System and has been unambiguously detected or inferred in every planet and/or their moon(s) where good spectroscopic data has been obtained.

In addition to water ice, other molecular solids have been observed in the solar system using spectroscopic methods. Solid carbon dioxide is found on all systems beyond the Earth except Pluto, although CO_2 sometimes appears to be trapped in other solids rather than as an ice on some objects. The largest deposits of carbon dioxide ice are found on Mars. Sulfur dioxide ice is found in the Jupiter system. Nitrogen and methane ices are common beyond the Uranian system.

Saturn's moon Titan probably has the most complex active extra-terrestrial surface chemistry involving organic compounds. Some of the observed or inferred compounds include ices of benzene (C_6H_6), cyanoacetylene (HC_3N), toluene (C_7H_8), cyanogen (C_2N_2), acetonitrile (CH_3CN), water (H_2O), carbon dioxide (CO_2), and ammonia (NH_3). Confirming compounds on Titan is hampered by its thick smoggy atmosphere, where in relative terms the atmospheric interferences that hamper surface characterization lie between that of Venus and Earth.

In this chapter we exclude discussion of the planets Jupiter, Saturn, Uranus, and Neptune because their thick atmospheres preclude observing the surface, even if surfaces exist. However, we do discuss spectroscopic observations on a number of the extra-terrestrial satellite bodies. Ammonia was predicted on many icy moons but is notably absent among the definitively detected ices with possible exceptions on Charon and possible trace amounts on some of the Saturnian satellites. Comets, storehouses of many compounds that could exist as ices in their nuclei, have only had small amounts of water ice definitively detected on their surfaces from spectroscopy. Only two asteroids have had a direct detection of surface water ice, although its presence can be inferred in others.

INTRODUCTION

The remote detection, identification, and mapping of materials using spectroscopy and imaging spectroscopy has been a rapidly advancing and maturing science over the last two decades, and promises significant advances into the future. Spectrometers and imaging spectrometers are now flying on many spacecraft throughout the Solar System, providing a wealth of new data that has led to many new discoveries. As of this writing, spectrometers and imaging spectrometers are in orbit or have recently flown past Mercury, Venus, Earth, Earth's Moon, Mars, several asteroids, Jupiter, Saturn, and on the way to Pluto. Aircraft-based sensors also play a key role in terrestrial imaging spectroscopy. This chapter will give a few examples of this very large and diverse field. The information is so vast, that the analogy for this chapter will be like taking a drink from Niagra Falls, thus we can cover only a small portion of the field. In order to limit the scope of this chapter, we limit discussions to spectroscopy of reflected solar radiation and thermally emitted light, and mostly exclude gamma-ray or radio wavelength spectroscopy. We only discuss remote detections across space (fly-by or orbiting spacecraft or in the case of the Earth, high altitude aircraft, above about 15 km). We exclude surface landers on other moons and planets.

Spectroscopy is a tool that has been used for decades to identify, understand, and quantify solid, liquid and gaseous materials, especially in the laboratory. In disciplines ranging from astronomy to chemistry, spectroscopic measurements are used to detect absorption features due to specific chemical bonds or electronic transitions, with detailed analyses used to determine the abundance and physical state of the detected absorbing species. Spectroscopic measurements have a long history in the study of the Earth and planets (e.g., Hunt 1977; Goetz et al. 1985; Pieters and Englert 1993; Clark 1999, Clark et al. 2003, 2007).

Reflectance and emittance spectroscopy of natural surfaces are sensitive to specific chemical bonds and transitions in materials, whether solid, liquid or gas. Spectroscopy has the advantage of being sensitive to both crystalline and amorphous materials, unlike some diagnostic methods, like X-ray diffraction. Spectroscopy's other main advantage is that it can be used up close (e.g., in the laboratory) to far away (e.g., to look down on the Earth, or up at other planets). Spectroscopy's historical disadvantage for materials identification is that it is sometimes too sensitive to small changes in the chemistry and/or structure of a material. The variations in material composition often cause shifts in the position and shape of absorption bands in the spectrum. Thus, with the vast variety of chemistry typically encountered in the real world, spectral signatures can be quite complex and sometimes unintelligible. However, that is now changing with increased knowledge of the natural variation in spectral features and the causes of the shifts. As a result, the previous disadvantage is turning into a huge advantage, allowing us to probe ever more detail about the chemistry of our natural environment (Pieters and Englert 1993; Clark 1999, Clark et al. 2003, 2007, 2013 and references therein).

Spectroscopic remote sensing from space, or high altitude aircraft requires the detection of reflected solar radiation at shorter wavelengths or thermally emitted light at longer wavelengths. The transition of predominantly reflected solar to predominantly emitted thermal radiation varies as a function of distance from the sun, and the object's albedo. The transition from reflected solar to emitted thermal emission occurs at approximately 1.5 μm at Mercury, 2.5 μm for our Moon, 3 μm for the Earth, 3.5 μm for Mars, ~6 μm for Jupiter's satellites, ~7 μm for Saturn's satellites, and beyond about 10 μm for the Neptune system (e.g., see Clark 1979).

Ice is probably the most abundance single mineral found in the Solar System. Ice technically refers to the mineral ice, solid H_2O, that is found naturally on the Earth. In the planetary sciences "ice" has become known as any volatile material that is frozen. Thus, in the planetary literature we discuss water ice, CO_2 ice, SO_2 ice, benzene ice, methane ice, etc. This chapter will also review such ices found on the surfaces of planets, their satellites, and small bodies in the Solar System.

The major elements that formed the solar system were hydrogen, carbon, nitrogen, and oxygen, often referred to as CHON material. When chemically combined, these elements produce molecules with low condensation temperatures—volatiles—with H_2O being the most refractory of these. Sulfur can also contribute to the volatile inventory, and the abundances of CHON + S material can be appreciable. The inferred molar elemental abundances present in the protoplanetary nebula, relative to hydrogen, of O, C, N, and S are 0.085, 0.036, 0.011, and 0.002, respectively (Anders and Grevesse 1989).

Under the reducing conditions produced by the presence of H_2, the expected closed-shell molecules are H_2O, CH_4, NH_3, and H_2S and these are observed as volatile gases or condensates in the atmospheres of the giant planets. Depending on thermal and chemical conditions in protoplanetary and protosolar nebulae, some or all of the above molecules, as well as those formed in more oxidizing conditions, will be incorporated in the forming satellites, comet nuclei, and dwarf planets. Examples of some stable volatiles formed under oxidizing conditions are CO, CO_2, N_2, and SO_2. Minor species may include CH_3OH, HCN, HCNO, etc. These volatiles condense in varying proportions at rates that are highly dependent on temperature and molecular interaction energies, ultimately forming the diverse ices that are found on outer solar system bodies.

In their pure states, molecules can condense in crystalline or amorphous forms, with crystalline compounds exhibiting a variety of polymorphs. The occurrence of a particular phase depends on the formation conditions, particularly the temperature and starting state (gaseous or liquid), and the subsequent thermal and irradiation history. For example, the freezing of liquid water produces hexagonal ice whereas amorphous, cubic, or hexagonal ice can be produced by condensation of the vapor at different temperatures.

Most minerals on and within solar system bodies are not pure, but contain other minerals or impurities. These mixed minerals can exist in many forms. The minor constituent can be randomly dispersed as isolated molecules within the crystalline or amorphous matrix (a solid solution). These molecules can be substitutional or interstitial, or trapped within defects or closed channels, sometimes existing as micro-atmospheres in voids (e.g., spectroscopically interacting O_2 molecules in H_2O ice, (Johnson and Jesser 1997; Loeffler et al. 2006) or CO_2 gaseous inclusions in minerals.

Closer to the sun, where temperatures in the solar nebula were hotter, rock forming minerals condensed in greater abundances. The solid surfaces of the terrestrial planets, Mercury, Venus, Earth and Mars are dominated by silicate and basaltic mineralogies and their weathering products.

DETECTION OF MINERALS AND THEIR
SPECTRAL PROPERTIES

The main method for remotely detecting minerals and compounds is by studying sunlight reflected from the surface under study (reflectance spectroscopy), and/or the heat emitted in the thermal infrared (thermal emission spectroscopy). Materials absorb light at specific characteristic wavelengths, thus spectroscopy can be used to directly and unambiguously detect a compound (given sufficient spectral range, resolution and signal-to-noise ratio). Other methods of remote sensing, such as neutron absorption only sense the presence of atoms, so do not directly detect a specific chemical compound, and require instrumentation in close proximity to the surface (e.g., low orbit). Reflectance and emittance spectroscopy, however, can be used to probe surfaces both near and to the outer reaches of the Solar System from the Earth's surface as well as from spacecraft. See Clark (1999) for a review of the different types of transitions and vibrations that lead to absorption features in spectra.

While absorption features are diagnostic of material identities, it is the scattering processes that control the light returned from a surface to a detector. Scattering occurs from mineral-vacuum (or gas) interfaces, grain boundaries or crystal imperfections, or from discrete impurities mixed in the surface of a material such as a particulate coating. In order to make an unambiguous detection of a particular material there must be a high enough intensity signal returned to the detector over a sufficient spectral range and with sufficient resolution to resolve diagnostic spectral features. Figure 1 illustrates the issue of sufficient spectral resolution for three operational terrestrial sensors compared to a laboratory spectrum.

A significant problem in detecting materials from space using reflected sunlight is correction of remotely sensed data for effects of the solar spectrum, and absorption and scattering from any atmosphere between the surface and spectrometer. Figure 2 gives an example. Remotely sensing surface composition through such an atmosphere poses challenges. The atmospheric transmission and scattering effects must be accurately corrected, however the atmospheric models are still evolving and correction methods are complex. Clark et al. (2002, 2003) discusses various methods for correcting terrestrial imaging spectroscopy data. Transmission and aerosol scattering is a significant problem on only 4 bodies in the Solar System where we can observe the surface: Venus, Earth, Mars, and Titan, Venus being the most difficult. Model transmissions for the Earth, Mars and Titan are shown in Figure 3. The mid-infrared transmittance of the Earth's atmosphere is shown in Figure 4, which shows even less transmission, mostly due to absorption by water.

Another problem in remotely sensing compounds is that the apparent strength of spectral features changes with grain size of the material. Not only do the absorption features change shape, the overall shape of the spectrum can also change. This is illustrated in Figure 5 with Ice.
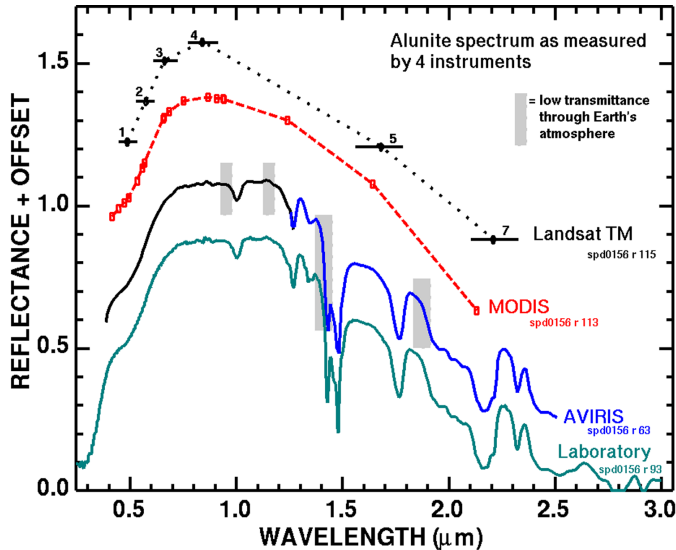
Figure 1. Comparison of sensors with different spectral resolutions. Landsat TM with 6 bands in the visible to near-infrared spectrum cannot resolve any absorptions typical in minerals. The MODerate resolution Imaging Spectrometer (MODIS) has enough spectral channels to barely resolve some spectral features in the visible portion of the spectrum, but not in the important near-infrared. The Airborne Visible and Infra-Red Imaging Spectrometer (AVIRIS), however, has sufficient spectral range and resolution to resolve many common absorption bands found in a wide variety of minerals and other compounds. The gray bands on the AVIRIS spectrum represent regions of the terrestrial atmosphere with strong absorptions. The spxnnnn entries are U.S. Geological Survey spectral IDs. Adapted from data in Clark (1999) and Clark et al. (2007).
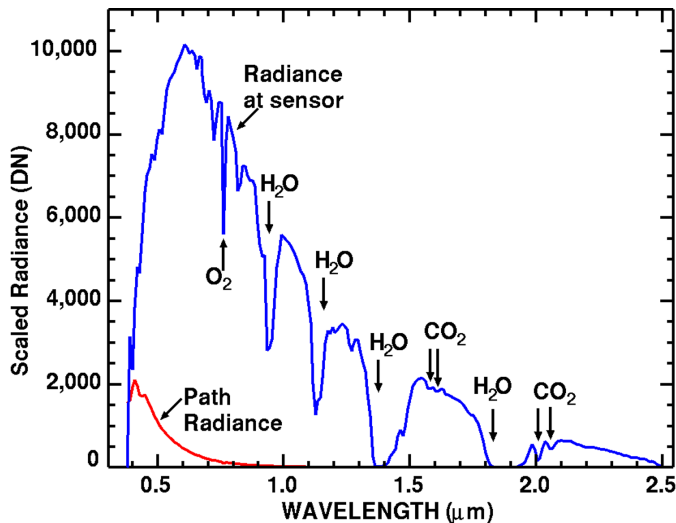

Figure 2. Observed signal of sunlight reflected from the Earth's surface measured at a height of 20 km by AVIRIS. The red line is the derived path radiance from the signal, light scattered by the atmosphere in the direction of the detector. To derive a surface reflectance spectrum, the solar spectrum, path radiance, and atmospheric absorption needs to be removed. DN stands for "Data Number" and is a relative scale. From Clark et al. (2002).
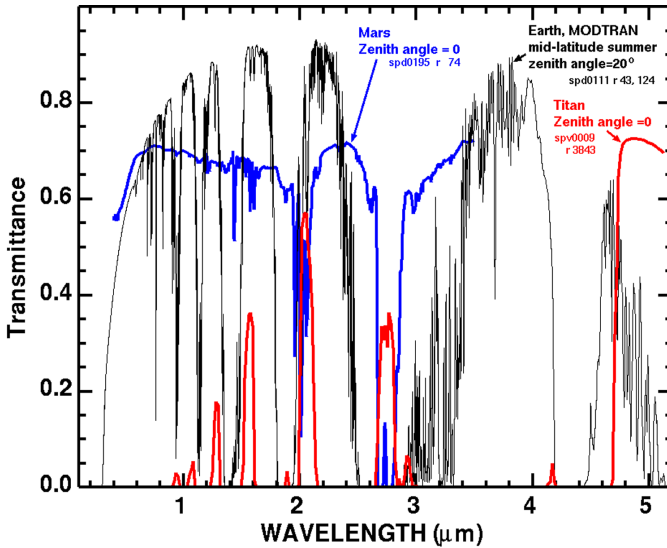
Figure 3. Model 1-way atmospheric transmission spectra for the Earth, Mars, and Titan. The dominant absorption in the Earth's atmospheric transmission is water vapor, with ozone providing the UV drop. The dominant absorption in Mars' atmospheric transmission is carbon dioxide and dust aerosol absorption plus scattering. The dominant absorption in Titan's atmospheric transmission is methane and hydrocarbon aerosol absorption plus scattering. Earth spectrum from Clark (1999), Mars from P. Irwin (personal communication, 1997), and Titan from Clark et al. (2010a). The transmission of Venus' atmosphere would be too low to register on this plot; transmission at 1 μm is <~ 0.00002 (Baines et al. 2000).
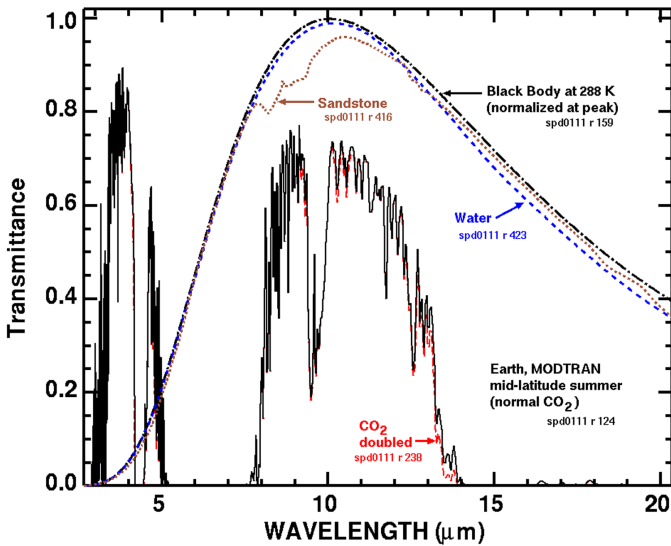

Figure 4. Atmospheric transmittance in the mid-infrared is compared to scaled grey-body spectra. Most of the absorption is due to water. Carbon dioxide has a strong 15-μm band, and the dotted red line shows the increased absorption due to doubling CO_2. Also shown is the black-body emission at 288 K and the grey-body emission from water and a sandstone scaled to fit on this transmittance scale. The water and sandstone curves were computed from reflectance data using: 1 - reflectance times a black-body at 288 Kelvin. Adapted from Clark (1999).
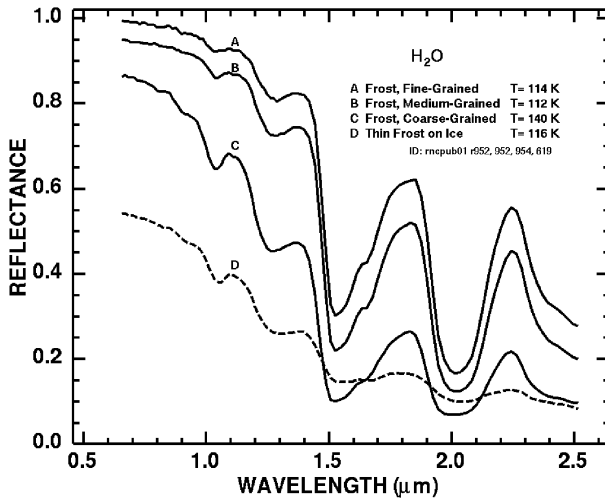
Figure 5. Illustration of changing ice absorption band shapes and strengths with grain size. The near-infrared spectral reflectance of A) a fine grained (~200 μm diameter) water frost, B) medium grained (~300 μm) frost, C) coarse grained (400-2000 μm) frost and D) an ice block containing bubbles and frost on the surface. The larger the effective grain size, the greater the mean photon path that photons travel in the ice, and the deeper the absorptions become. Curve D is very low in reflectance because of the large path length in ice but scattering from fine frost at the surface raises the reflectance. Adapted from data in Clark (1981), and Clark and Lucey (1984) with level corrections from the reflectance standard.

Spectroscopic characterization of minerals is well-covered in Pieters and Englert (1993), Clark (1999), and Clark et al. (2007), and references therein. Detection strategies are discussed in Clark et al. (2003) and references therein. Spectroscopy of ices are reviewed in Clark et al. (2013) and more briefly below.

Detection of a particular mineral on a planetary surface is only one aspect of understanding the geology and chemistry of the surface. Mapping the locations and geologic context greatly enhances our understanding of planetary surfaces, including their origin. Mapping solid and liquid compounds on a planetary surface is accomplished with imaging spectrometers. There are several types of imaging spectrometers. Two widely used diffraction grating types include whiskbroom scanners which collect spectra in a cross-track manner by using an oscillating mirror to sequentially reflect light from each spatial location in a scene to a spectrometer one pixel at a time, and pushbroom scanners which measure the spectra of all the pixels across an image simultaneously using an area array detector and the forward motion of the spacecraft. Whiskbroom scanner data are more easily calibrated because the same detector array measures the spectrum of every pixel in the scene, but dwell time on a given pixel is relatively short so images can be noisy. Pushbroom scanners have longer dwell times on each pixel so provide a less noisy image, but images are commonly plagued by along-track image artifacts caused by miscalibration of adjacent pixel array elements. See Goetz et al. (1985) and Clark et al. (2003) for more details. Whiskbroom systems include the NASA JPL classic Airborne Visible/Infrared Imaging Spectrometer (AVIRIS), flown on high altitude aircraft above the Earth (Green et al. 1990) and the NASA Visual and Infrared Mapping Spectrometer (VIMS) currently orbiting Saturn (Brown et al. 2005a). Pushbroom imaging spectrometers include the Compact Reconnaissance Imaging Spectrometer for Mars (CRISM) (Murchie et al. 2007) which is currently orbiting Mars on the Mars Reconnaissance Orbiter (MRO). Broadband imaging systems like the Mars Themis (Christensen et al. 2004) and HiRISE (McEwen et al. 2007) are not discussed because they are not spectrometers, nor imaging spectrometers.

MINERAL AND FROZEN VOLATILES SPECTRAL SIGNATURES

H₂O (ice)

Water ice phases and spectral features as a function of temperature are discussed in detail by Mastrapa et al. (2013). Ice forms multiple crystal structures, including cubic (Ic), hexagonal (Ih), and amorphous solids (Hobbs 1975 and references therein) which might be encountered on planetary surfaces in the solar system. The spectra of crystalline water ice (Fig. 5, and see Grundy and Schmitt 1998) display particularly broad absorptions because the water molecules are orientationally disordered. In hexagonal or cubic ice, the oxygen atoms are in a well-defined crystal structure, but the hydrogen bonds point randomly toward neighboring oxygen atoms.

Mastrapa et al. (2008) measured the optical constants of crystalline and amorphous ice from 20 to 120 K and reviewed formation conditions for amorphous versus crystalline water ice. Below about 135 K, amorphous ice is expected to condense from the vapor phase if the rate of growth is slow. Thus, we might expect amorphous ice to be present in the Jupiter system and beyond. However, as we will see, with the probable exception of the Jupiter system, where surfaces are being irradiated by particles caught in Jupiter's magnetic field, outer solar system surfaces are dominated by crystalline H_2O.

In amorphous ice, the absorptions shift to shorter wavelengths. The Fresnel peak near 3.1 μm also shifts to shorter wavelengths, and the temperature sensitive 1.65-μm absorption becomes very weak. See Clark et al. (2013).

SO₂ ice

SO_2, a colorless gas at room temperature, is a common terrestrial volcanic (and industrial) effluent and also present in Venus's atmosphere, possibly from recent volcanic activity. It is the major component emitted from Jupiter's volcanically active moon Io. SO_2 is a bent molecule of the form O-S-O and is a stable sulfoxide, with SO and S_2O being much less stable. Oxidation of SO_2 in the presence of H_2O produces sulfuric acid, evident in the Earth's atmosphere as acid rain and in Venus's atmosphere as the ubiquitous sulfuric acid clouds and haze.

SO_2 is more refractory than NH_3, it liquefies at ~263 K and freezes at ~200 K. Within the temperature range of 90 K to 120 K, appropriate for Jovian satellites, the SO_2 vapor pressure varies by five orders, from about 10^{-4} nbar to 10 nbar. SO_2 is amorphous when condensed at temperatures < 70 K, but crystallizes at temperatures > 70 K (Schmitt et al. 1994). Condensed SO_2 forms many different textures (Nash and Betts 1998). The condensation, evaporation, and metamorphism of pure SO_2 and mixed ices have been discussed by Sanford and Allamandola (1993).

Useful reviews of SO_2 properties by Schmitt et al. (1998b) and Nash and Betts (1998) are found in the Solar System Ices book (Schmitt et al. 1998a). Infrared and ultraviolet spectroscopy of SO_2 is summarized in Carlson et al. (2007).

Nitrogen ice (N₂)

Although nitrogen is cosmochemically abundant, the high volatility of N_2 ice makes it unstable except at extremely low temperatures characteristic of the outer edge of the Solar System. There are two low-pressure phases of N_2 ice. Above 35.61 K, the stable form is beta N_2 ice, an orientationally-disordered hexagonal close packing solid (Scott 1976). It is difficult to detect spectroscopically, because N_2 is a non-polar molecule in which vibrational absorptions are not easily excited. Only when an N_2 molecule collides with another molecule is a dipole moment temporarily induced, enabling a photon around 4.25 μm to excite its 1-0 fundamental vibrational mode (e.g., Shapiro and Gush 1966; Sheng and Ewing 1971). This collision-induced absorption is relatively broad (~100 cm⁻¹ in wavenumber units), compared with gas-phase absorptions due to fixed dipole moments, owing to the modulation of the vibrational transition by the translational motion of the colliding pair. See Clark et al. (2013) for further review and references.

Hydrocarbons and other ices

Hydrocarbons are a diverse category of organic compounds, comprising numerous families without heteroatoms and with functional groups of solely hydrogen and carbon atoms. The simplest hydrocarbons are the alkanes – singly bonded molecules with no reactive functional groups. Hence, they tend to combust at relatively high temperatures, even though they are composed entirely of low atomic weight atoms, and have a generic chemical formula of C_nH_{2n+2}. If the carbon backbone contains a C-C double bond, the hydrocarbon is termed an alkene, and it has a formula of C_nH_{2n} (e.g., propene, C_3H_6); with a C-C triple bond, it is called an alkyne whose formula is C_nH_{2n-2} (e.g., propyne, C_3H_4). In the singly bonded alkanes, hydrogen atoms will bond to all the remaining positions on the carbon atom, and they are known as saturated hydrocarbons. Unsaturated hydrocarbons then, are those with doubly or triply bonded carbon atoms, and they will have less than their 'full' complement of hydrogen atoms. Together, these straight (or branched) chain hydrocarbons are known as 'aliphatic' compounds, and also include such derivatives as fatty acids (Wade 2005).

In general, spectra of different families share different spectral characteristics while spectral properties are similar within a family (also called group or series). For example, Figure 6 shows spectral differences among ices in the alkane, alkene, and alkyne groups from Clark et al. (2009). In alkanes, the C-H stretch fundamental occurs near 3.4 μm, whereas in the C-C double bonded alkenes, the C-H stretch shifts closer to 3.2 μm, and in the C-C triply bonded alkynes, the C-H stretch shifts to nearly 3.0 μm (Fig. 6).

The carbon skeleton can close in on itself in two ways: by creating a ring of singly-bonded carbon atoms of any length equal to or greater than three (cycloalkanes, known as alicyclic hydrocarbons), *or* by the overlapping of p orbitals from adjacent carbon atoms into pi (π) bonds to create a benzene ring (C_6H_6). The benzene ring with overlapping *p* orbitals is particularly stable, and forms the basis of the aromatic hydrocarbon family.

Most organic molecules are infrared active, displaying absorption features associated with stretching and bending vibrations. For example, the C-H stretch fundamental of aromatic
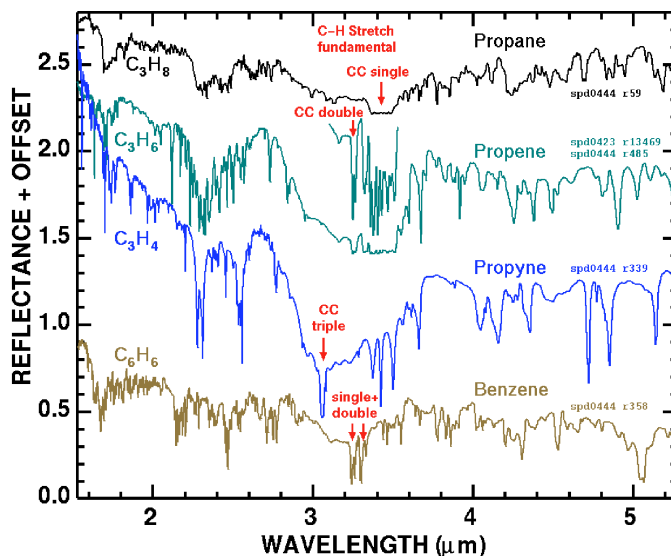

Figure 6. Reflectance spectra of propane, propene, propyne and benzene ices. From Clark et al. (2009).

hydrocarbons occurs near 3.3 µm (Fig. 6) and a bending mode absorption has been used to detect benzene ice on Saturn's moon Titan. Because these transitions are specific to the atoms and their chemical bonds, and are similar regardless of the type of larger molecule within which they are contained, an examination of the IR spectrum will reveal an enormous amount of information about an unknown compound (e.g., as seen in Fig. 6). Clark et al. (2009) observed that the spectral complexity of organic ices first increases as molecular weight increases, then decreases at higher molecular weights. The loss of spectral structure at high molecular weights is probably due to many overlapping absorptions averaging out small details.

Methane ice (CH_4)

Methane deserves special attention as the smallest and simplest alkane, as well as being the hydrocarbon most widely observed as an ice on solar system bodies. It is readily detected spectroscopically by means of numerous overtones and combinations of four fundamental vibrational transitions. These are a symmetric mode $v_1(A_1)$ at 2914 cm^{-1} (3.43 µm), a doubly degenerate $v_2(E)$ bending mode at 1526 cm^{-1} (6.55 µm), and triply degenerate stretching $v_3(F_2)$ and bending $v_4(F_2)$ modes at 3020 and 1306 cm^{-1} (3.31 and 7.66 µm), respectively (Grundy et al. 2002). Two different condensed phases occur at zero pressure. At temperatures below 20.4 K, CH_4 exists as a cubic crystal, whereas above that temperature, it loses its orientational order and long-range coordination, resulting in broadened bands similar to (but not identical to) those of liquid methane (e.g., Ramaprasad et al. 1978; Martonchik and Orton 1994). Temperature-dependent spectra have been measured for methane ice between 0.7 and 5 µm, revealing subtle changes with temperature that offer an as-yet unexploited potential for remote sensing of CH_4 ice temperatures (Grundy et al. 2002). Methane molecules dispersed in nitrogen ice exhibit slightly different spectral behavior, characterized by subtle wavelength shifts toward blue wavelengths as well as the loss of a weak transition at 1.69 µm (Quirico et al. 1997b). This property provides a way to remotely distinguish diluted from pure CH_4, as well as the potential to detect smaller quantities of nitrogen ice than can be readily detected through observation of the much weaker N_2 ice absorptions, with specific applications discussed later in this chapter.

MINERALS AND COMPOUNDS IN THE SOLAR SYSTEM DETECTED WITH SPECTROSCOPY

We will now discuss the detections of minerals and other compounds on planets and their satellites in our Solar System.

Terrestrial planets

Mercury. Vilas et al. (2012), Izenberg et al. (2012), and Riner and Lucey (2012) have searched for spectral features in the MErcury Surface, Space Environment, GEochemistry, and Ranging (MESSENGER) spacecraft data of the planet Mercury. To date, no plausible spectral features for identifying mineralogy, for example, pyroxene absorptions like those seen on the Moon have been found. It appears that the surface of Mercury is intensely space-weathered, where the surface minerals are partially destroyed, leaving rinds enriched in nano-phase metallic iron. See Hapke (2001) and Chapman (2004) for more on terrestrial space weathering, and Clark et al. (2012) for space weathering effects in the outer solar system.

Venus. Venus has a thick highly scattering atmosphere, making it the most difficult surface to be detected from space (excluding Jupiter, Saturn, Uranus, and Neptune whose surfaces, if they exist are impossible to see with UV to far infrared light). Three spacecraft have detected thermal emission from the surface using near-infrared wavelengths: Galileo NIMS (Carlson et al. 1991), Cassini VIMS (Baines et al. 2000), and Venus Express VIRTIS (Müller et al. 2008, Titov et al. 2009 and references therein). Baines et al. (2000) showed that it could be possible to use a few windows in the Venetian spectrum to detect broad electronic absorptions due to iron

in surface minerals and Hashimoto et al. (2008) have used these windows and suggested felsic materials in Venus's highlands.

Earth. The Earth is the only planet whose temperature is near the melting point of water where both liquid and solid water exists on the surface. This condition enables a complex hydrologic cycle of both solid and liquid water eroding, reshaping and weathering the surface. Active plate tectonics recycles crustal minerals, and creates active volcanism which leads to a variety of important mineral-forming conditions. Over three thousand minerals have been found naturally occurring on the Earth (e.g., Fleischer and Mandarino 1995). Dozens of minerals have been detected at the Earth's surface using spectroscopy from high-altitude aircraft (e.g., the NASA JPL Airborne Visible/Infrared Imaging Spectrometer, AVIRIS), commercial aircraft spectrometers, and spacecraft. The Earth's high carbon and nitrogen environment, energy sources, and hydrologic cycle provide a unique surface composition with abundant water, organic compounds, and life. The Earth's surface is dominated by liquid water, solid water, vegetation, and, in some locations, minerals in exposed rocks and soils.

While there are many imaging spectrometers on the way to, or have recently flown by or orbited, or are currently orbiting planets and satellites throughout the Solar System, very oddly there is only one (non-military) true imaging spectrometer in orbit around the Earth, the aging EO-1 Hyperion system (e.g., Barry et al. 2001). Because the Hyperion instrument is relatively old and its near-infrared performance is significantly lower than that of aircraft systems, many studies rely on systems like the NASA JPL Airborne Visible/Infrared Imaging Spectrometer (AVIRIS) system (Green et al. 1990) and other commercial systems which fly at lower altitudes.

The number of terrestrial applications of spectroscopy from space or aircraft is stunning, ranging from mineral mapping (e.g., Clark et al. 2003 and references therein) as shown in Figures 7a and 7b, acidic mine drainage and mineralization impact (e.g., Swayze et al. 2000), ecosystems mapping, vegetation species and chemistry (e.g., Kokaly et al. 2003; Clark et al. 2003; Ustin et al. 2009 and references therein), ice and snow mapping, including snow grain size and snow-water-vegetation mixtures (e.g., Clark et al. 2003; Painter et al. 2003 and references therein), mapping chlorophyll in water (Clark et al. 2003; Clark and Wise 2011), assessments of environmental disasters (the World Trade Center Disaster: Clark et al. 2001, 2006; the 2010 Gulf of Mexico Deepwater Horizon oil spill: Clark et al. 2010b), and detection of fires/thermal hot spots through thick smoke, determining temperature and sub-pixel areal extent (Clark et al. 2003, 2006). Remote sensing had been tried for decades to derive a method to determine the amount of oil on the ocean's surface without much success. But in the most recent disaster, the Gulf of Mexico 2010 oil spill, by using absorption features in oil and the spectral resolution of AVIRIS, Clark et al. (2010b) simultaneously solved for the oil:water ratio of intimate mixtures (e.g., water-in-oil emulsions), thickness of the mixture and their sub-pixel areal fraction to derive oil volume per pixel. Such unmixing is only possible using the many wavelengths provided by a visible to near-infrared imaging spectrometer.

The Earth's Moon. Water ice is thought to exist in the permanently shadowed craters on the moon and neutron spectrometer data from Lunar Prospector (Feldman et al. 1998, 2000, 2001) showed that hydrogen is present in the lunar polar regions. More recently Clark (2009), Pieters et al. (2009), and Sunshine et al. (2009) reported that adsorbed water is extensive in the lunar surface raising the likelihood that some of it has migrated and is trapped in the polar regions. Coleprete et al. (2010) reported detection of water vapor and water ice in the ejecta from the NASA LCROSS impact into South Pole crater Cabeus A. They also claim detection of other volatile compounds. Paige et al. (2010) reported temperatures as low as 38 K in Cabeus A, where many volatile compounds might exist as ices.

The Chandrayaan-1 spacecraft with the Moon Mineralogy Mapper (M^3) is the only imaging spectrometer to orbit the Moon covering the reflected solar spectral range. The M^3 instrument
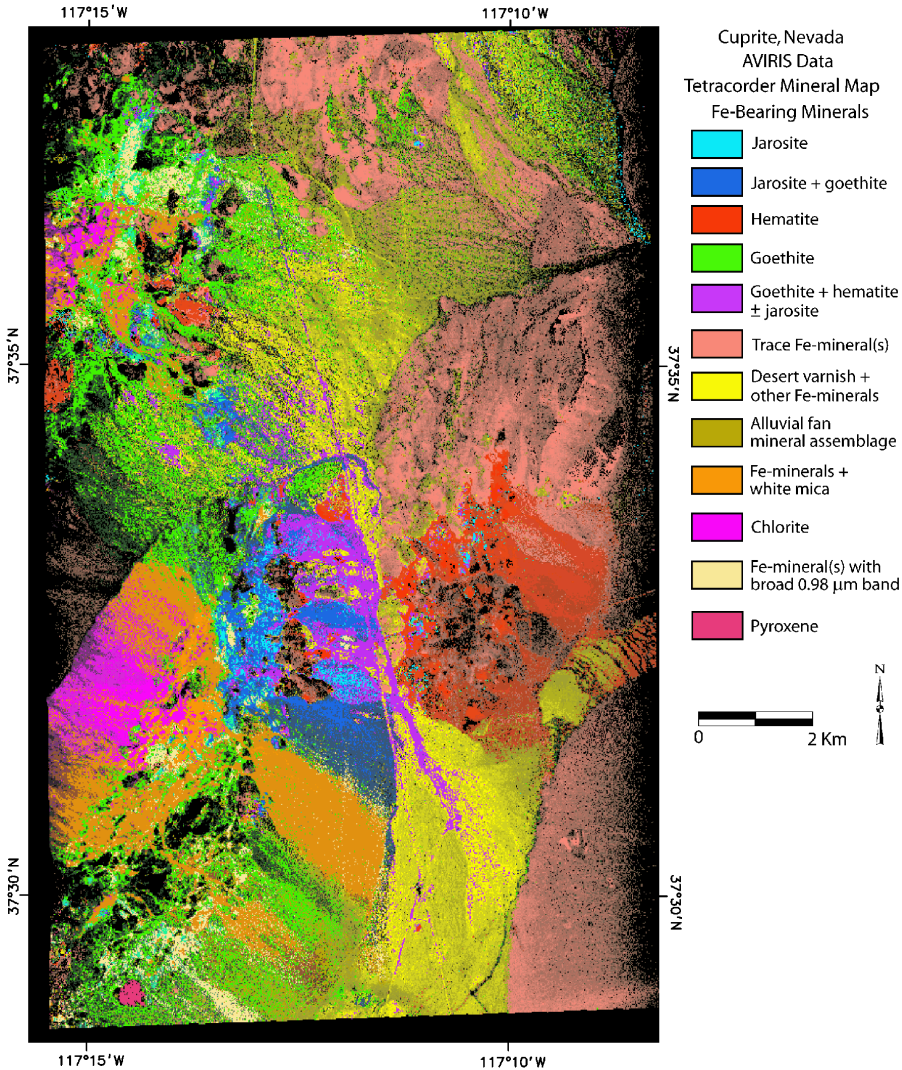
Figure 7. (a) Imaging spectroscopy mapping results from AVIRIS imaging spectrometer data over Cuprite, Nevada for absorptions in the 1-μm spectral region due to Fe^{2+} or Fe^{3+}. All the Fe^{2+} - Fe^{3+} absorptions overlap making separation difficult. Yet through spectroscopic analysis, not only can the minerals be distinguished, but mixtures could be distinguished based on the shape of the overlapping absorption features. From Swayze et al. (2003) with modifications.

has been used to detect and map a variety of minerals on the Moon, including the pyroxene solid solution series, olivines, feldspars and spinels (e.g., Pieters et al. 2011 and references therein). Kramer et al. (2011) showed an interesting link between the enigmatic lunar swirls which seem to lack hydroxyl that occurs in the surrounding rocks and soils.

Mars. Orbital high spectral resolution mapping of Mars over the last two decades with the Thermal Emission Spectrometer (TES) on Mars Global Surveyor (Christiansen et al. 1992), Observatoire pour la Minéralogie, L'Eau, les Glaces et l'Activitié (OMEGA) on Mars Express
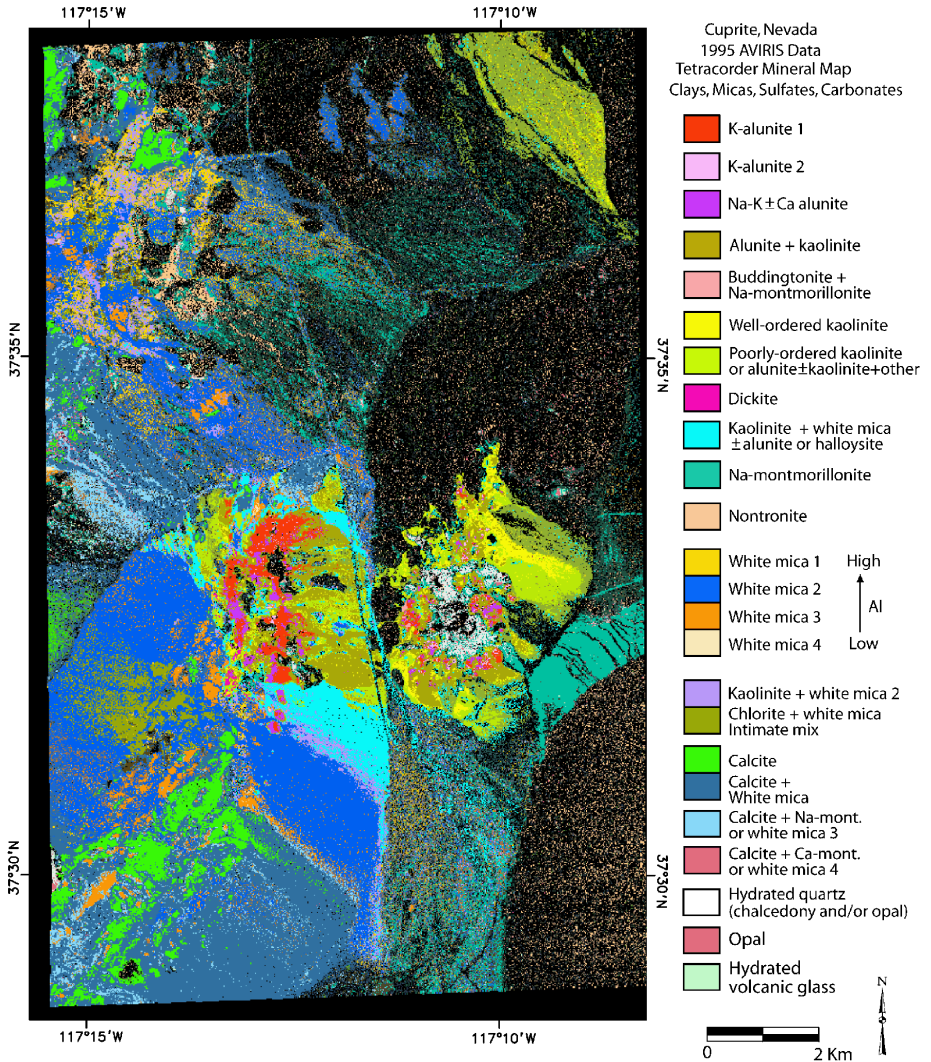
Figure 7. (b) Imaging spectroscopy mapping results from AVIRIS imaging spectrometer data over Cuprite, Nevada. The results distinguish kaolinite, alunite, carbonate, mica and other minerals, separate kaolinite from alunite-dominated areas, and also indicate where both occur as mixtures. From Swayze et al. (2003) with modifications.

(Bibring et al. 2004a), and the Compact Reconnaissance Imaging spectrometer for Mars (CRISM) on the Mars Reconnaissance Orbiter (Murchie et al. 2007) has led to numerous discoveries of mineral phases on the surface. One of the main goals that these imaging spectrometer share is the search for minerals formed during the early part of Martian history when water existed temporarily at the surface and for longer periods at depth. The spectral signatures of minerals frequently provide information about their environment of formation. Some minerals hint at metamorphic processes caused by elevated temperature and pressure caused by impacts. Clays and evaporites require water to form and are sensitive to formative pH conditions that can influence the preservation of fossils. Kaolin group minerals and the sulfate mineral alunite

may indicate the past presence of hydrothermal activity around hot spring deposits or acidic paleolakes. In this way, spectroscopists can use orbitally detected minerals as proxies to focus rover missions on the most promising sites in the search for evidence of past life.

During its operation from 1996 to 2006 the TES interferometer, which measured mid-infrared wavelengths for 3 km pixels on the surface, was used to discover concentrations of hematite in Meridiani Planum (Christensen et al. 2000), leading to its selection as a landing site for the Mars Exploration Rover Opportunity. Other mineralogic discoveries include olivine in Nili Fossi (Hoefen et al. 2003), globally distributed pyroxene (Christensen et al. 2001), and possibly carbonate (Bandfield et al. 2003) and zeolite minerals (Ruff 2004) distributed globally in the Martian dust. Originally, Christensen et al. (2001) thought TES data indicated the presence of basalt in the southern highlands and more silica-rich andesite in the northern plains. Wyatt and McSween (2002) argued that these more silica-rich spectral detections are actually weathered basalts with thin coatings of silica glass. Nevertheless, TES may have revealed the presence of rare exposures of granitoid rocks in the central uplifts of two adjacent craters (Bandfield et al. 2004) suggesting the presence of mechanisms that can produce highly differentiated magmas.

OMEGA led the way in orbital visible – near infrared spectroscopic mineral discoveries on Mars with its typical 1-2 km pixel resolution. Detailed variations in Fe-pyroxene distribution were documented by Mustard et al. (2005). Gendrin et al. (2005) identified the monohydrated Mg-sulfate kieserite in layered deposits on the surface while gypsum-rich sand dunes were identified by Langevin et al. (2005) at circumpolar latitudes. Poulet et al. (2005) observed sparsely distributed phyllosilicates such as montmorillonite, Fe/Mg smectite, and nontronite consistent with an early stage of neutral to alkaline Martian hydrologic activity. Based on these and other mineral discoveries, Bibring et al. (2006) recognized several eras of mineralogic evolution on Mars: the "phyllocian" (~4.5 to 3.8 billion years ago) where aqueous alteration at more neutral pH formed phyllosilicates in the oldest terrain, the "theiikian" (~3.8 to 3.3 billion years ago) where sulfates were formed in a more acidic environment, and the "siderikian" (~3.3 billion years ago to the present) where anhydrous ferric oxides formed from slow weathering primarily in the absence of liquid water.

CRISM, the latest orbital visible-near infrared spectrometer to orbit Mars, is a pushbroom imaging spectrometer that has two data collection modes: a targeted hyperspectral mode that measures light from 0.36 to 3.92 μm over 544 spectral channels at a spatial resolution up to 18 m per pixel, and a multispectral imaging mode that collects subsets (e.g., 72, 94, or 262) of its 544 channels at a spatial resolution of 100 to 200 m per pixel (Murchie et al. 2007). The hyperspectral mode produces full spatial resolution 10×10 km hourglass-shaped images with 18 m pixels or half spatial resolution 10 x 20 km images with 36 m pixels. In targeted mode, CRISM spectral sampling is approximately 6.5 nm. CRISM is gimbaled so it can swivel to perform continuous spectral measurements on a target while the spacecraft flies over the location. This allows higher spatial and spectral resolution measurements to be obtained with better signal-to-noise ratios. Gimbaling also allows acquisition of up to 11 images of the same target at varying emission angles during an overpass to facilitate separating surface absorptions from atmospheric ones. Recently, CRISM began acquiring targeted hyperspectral images with along-track overlap to produce images with 3-12 m pixel resolution over the most interesting areas (e.g., rover sites).

CRISM data can be calibrated to apparent reflectance by first converting the data from instrument units to I/F (the ratio of the reflected intensity to the incident intensity of sunlight), next photometrically correcting it, then assuming Lambertian scattering applies, dividing it by the cosine of the incidence angle, and lastly correcting it for atmospheric gas absorptions by dividing by a scaled atmospheric transmission spectrum of Olympus Mons as explained in Mustard et al. (2008). Image noise can then be reduced using a filtering algorithm that

replaces outlier pixels in the spectral and spatial dimensions of the image cube (Parente 2008). Remaining noise is further reduced in each column by dividing individual pixel spectra by a spectral average calculated from pixels lacking narrow vibrational absorptions from that column. Alternatively, a DISORT-based radiative transfer model can be used to convert I/F data to surface Lambert albedo resulting in spectra nearly free of atmospheric gas artifacts (McGuire et al. 2008). This last method is compute intensive so has been applied to only a select group of CRISM scenes.

CRISM has allowed planetary scientists to leverage its fine pixel resolution to identify, in unprecedented detail, an even broader array of carbonates, phyllosilicates, opaline silica, sulfates, and zeolites on the Martian surface. Ehlmann et al. (2008) identified Mg-carbonate in the Nili Fossae region formed by alteration of olivine by hydrothermal fluids or near-surface water that were not destroyed by more acidic conditions later in Martian history. A number of researchers (Murchie et al. 2009; Mustard et al. 2008; Bishop et al. 2008; Noe Dobrea et al. 2010) have noted that extensive phyllosilicate-rich layers, in some cases hundreds of meters thick, blanket old eroded highland areas. At the highest spatial resolution, these layers resolve in places into a lowermost Fe/Mg-smectite unit, a middle montmorillonite unit, and an upper kaolinite-rich unit suggestive of a weathering profile as conditions became more acidic with time. Curiosity, the Science Laboratory rover, successfully landed in and has begun exploring Gale Crater where CRISM has identified diverse phyllosilicate and sulfate mineralogy in a 5 km high pile of layered rocks believed to have recorded climatic conditions during the first billion years of Martian history (Milliken et al. 2010). Gale crater is 152 km in diameter and is just 5º south of the equator. Stratigraphic exposure in the central mound is more than twice that of the Earth's Grand Canyon (Thomson et al. 2011). The rover will traverse the central mound examining the lowermost section and then upper portion to determine if these sediments record the progressive "drying out" of Mars.

Ehlmann et al. (2009) summarizes spectral evidence for nontronite, Mg-rich smectite, chlorite, prehnite, serpentine, kaolinite, K-mica, opaline silica, Mg-carbonate, and the Na-zeolite analcime in and around the Nili Fossae region. They suggest these minerals may indicate that low-grade metamorphism or hydrothermal aqueous alteration has occurred in this region in the past. Milliken et al. (2008) identified opaline silica on Mars based on CRISM spectra that were initially confused with the Al-rich smectite montmorillonite. Under terrestrial conditions opal has a broader 2.2-μm absorption compared to that of montmorillonite (Fig. 8). But under simulated Martian conditions weakly hydrogen bonded water normally present under relatively humid terrestrial conditions is lost causing the 2.2-μm absorption to narrow so it forms a better spectral match to CRISM spectra of widespread Martian surface rocks. Ehlmann et al. (2011) argue that spectroscopic evidence of minerals from assemblages formed under anoxic high temperature conditions, a high ratio of primary to secondary minerals, and observed stratigraphic relations indicate substantial amounts of clay formed by hydrothermal groundwater circulation and that cold, arid conditions with only transient surface water existed at the surface since the early Noachian period nearly 4 billion years ago. This explanation diminishes the need for an atmosphere thick enough to support persistent liquid water and clay formation by near-surface weathering (Bibring et al. 2006; Ehlmann et al. 2011).

Sulfate deposits on Mars are similarly detectable. Bishop et al. (2009) identified szomolnokite, a monohydrated Fe-sulfate in light-toned mounds within Valles Marineris and hydrated silica with hydroxylated ferric sulfate on the surround plateau. Lichtenberg et al. (2010) noted that a wide expanse of hydroxylated ferric sulfate underlies what is probably a layer of szomolnokite deposited as part of an evaporitic sequence in Arma Chaos. Several workers (Farrand et al. 2009, Milliken et al. 2008) have identified the yellow Fe-sulfate hydroxide jarosite in areas where water may have been present. Wray et al. (2011) used CRISM to map the distribution of a bathtub-ring of sulfates (i.e., gypsum, poly- and mono-hydrated
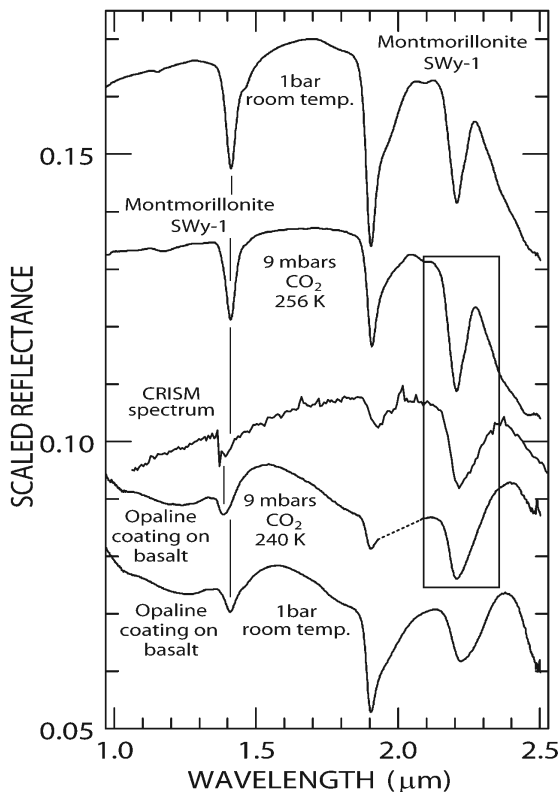
Figure 8. Laboratory spectra of montmorillonite and an opaline coating on a 3,000-5,000 year old basalt from Mauna Loa, Hawaii, at terrestrial conditions and simulated Martian surface conditions compared with an average of 120 spectra from MRO CRISM scene HRL000044AC collected over the plains around Valles Marineris south of Melas Chasma. Artifacts due to CO_2 have been replaced by the dashed line to facilitate spectral comparison. Box encloses CRISM spectrum and lab mineral spectra measured at simulated Martian conditions. Figure modified from Swayze et al. (2007).

Mg/Fe sulfates, and jarosite) and phyllosilicates (i.e., kaolinite, montmorillonite, and Fe/Mg-smectites) deposited as an evaporative scum by the receding waters of 900-meter deep paleolake that once partially filled Columbus Crater. Swayze et al. (2008) identified K-alunite in light toned layers on the floor of Cross Crater in the southern highlands in association with kaolinite, montmorillonite, and opal (Fig. 9). These minerals form partially concentric zones with alunite at the core suggestive of terrestrial relict acid-sulfate hydrothermal deposits. The relatively low-temperature (<100 °C) spectral signature of the alunite and its presence at the foot of the crater wall suggest it may have formed by precipitation in hydrothermal springs where acidic-water discharged into a lake that filled the crater to several hundred meters depth. Deposits in this crater and those in Columbus Crater would be excellent sites for future rover missions looking for evidence of past life.

As a general rule, the relative timing of phyllosilicate and sulfate deposition on Mars appears to be controlled by a progressively drying climate. Thollot et al. (2012) have found an exception, where a closed depression in the Noctis Labyrinthus region of Mars holds several hundred meters of stratified material enriched in phyllosilicates and sulfates, and both formed in situ during the Late-Hesperian epoch (3.4 to 3.0 billion years ago) after the Noachian period
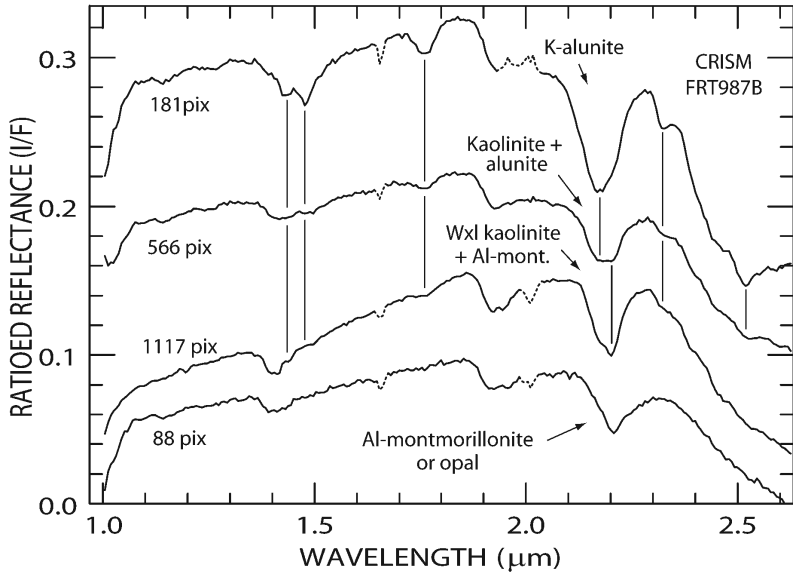
Figure 9. CRISM spectra of light-toned layered units on the floor of the 65 km diameter late Noachian Cross Crater in the southern highlands of Mars. Spectra were extracted from CRISM scene FRT0000987B; number of pixel spectra averaged listed at left end of each spectrum. Vertical lines mark position of diagnostic absorptions used to identify mineral phases and their mixtures. Wxl = well crystalline; Al-mont. = Al-montmorillonite. Figure modified from Swayze et al. (2008).

(4.1 to 3.8 billion years ago) when most phyllosilicates are thought to have formed. Their evidence suggests that the broadly diverse mineral assemblages formed from local volcanic activity and related hydrothermal alteration, and that geological setting may be just as important as geological timing when trying to understand orbitally detected mineral deposits.

Mars has seasonal and remnant polar caps of H_2O and CO_2 ices, as well as permafrost and geologic features indicative of glacial flow and sublimation of water ice from below the surface. Mars' seasonal polar caps extend down to about 50° latitude (e.g., James et al. 1993 and references therein). Due to present day obliquity, the southern hemisphere is drier than the northern hemisphere. The southern residual cap is dominated by CO_2 ice while the northern residual cap is dominated by H_2O ice (Farmer et al. 1976; Kieffer et al. 1976). However, it has recently been confirmed that an H_2O cap underlies the southern CO_2 remnant cap (Byrne and Ingersoll 2003; Bibring et al. 2004b).

More than 25% of the atmospheric CO_2 condenses each year to form the seasonal caps (Forget et al. 1995; Kieffer and Titus 2001). The NASA Phoenix lander and Mars Reconnaissance Orbiter, Compact Reconnaissance Imaging Spectrometer for Mars (CRISM), and the High-Resolution Imaging Science Experiment (HIRIS) instruments have quantified growth of the northern seasonal polar cap of H_2O and CO_2 at 68° N latitude (e.g., Cull et al. 2010; Fig. 10). During winter, the CO_2 ice grows to a depth of about 0.35 m with a thin layer of H_2O ice on the surface.

Asteroids and comets

Although asteroids generally show only silicate minerals on their surfaces, ice has been reported in two asteroids, 24 Themis (Rivkin and Emery 2008; Campins et al. 2009) and (65) Cybele (Licandro et al. 2011). Both objects have a weak absorption at 3-μm best described
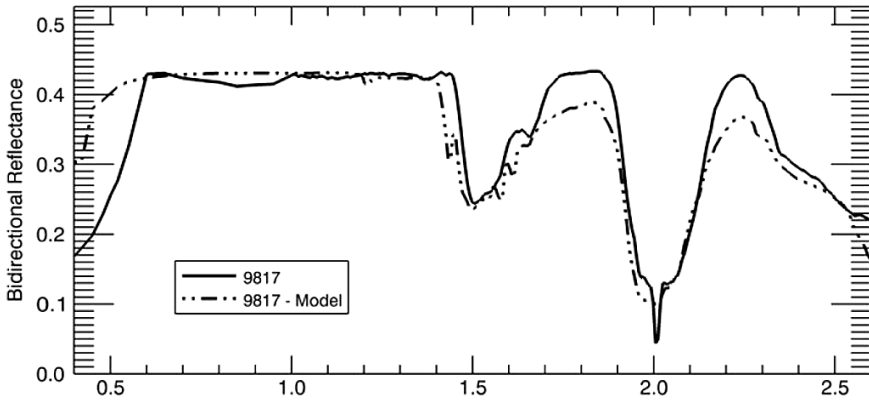
Figure 10. CRISM spectrum of the Mars Phoenix landing site (solid line) from orbit and model results (dotted lines) obtained at Ls~19.3°. Water ice dominates the spectrum with smaller amounts of CO_2 ice. The horizontal axis is the wavelength in microns. From Cull et al. (2010).

by water ice. However, strongly hydrogen bonded water can also display absorptions at the wavelengths where ice absorbs and higher signal-to-noise ratio spectra are needed to confirm this weak absorption. In addition, Themis has been reported to contain organic material (Campins et al. 2010; Rivkin and Emery 2010).

Comets are dark, with reflectances of only a few percent, and their surfaces are commonly thought of as carbonaceous lag deposits, the refractory remains left behind by the sublimation of dirty ice. While water is the major volatile species on comets, detection of water on the surface has been elusive. Davies et al. (1997) detected weak absorptions attributed to water ice in comet Hale-Bopp but the spectra included the coma. They also showed possible evidence for the ice being amorphous, but the low signal-to-noise ratio and weak absorption strength precludes a definitive detection when considering the far infrared spectrum of amorphous versus crystalline ice. Lellouch et al. (1998) also reported detection of ice in the coma of Comet Hale-Bopp. The temperatures they derived, 170 K, for their observations are too high for amorphous ice. A detection of ice on a comet nucleus without interference from the coma, comet Tempel 1, was reported by Sunshine et al. (2006) using the Deep Impact spacecraft where small exposures of ice were seen by the imaging spectrometer. The Deep Impact extended mission shows isolated patches of water ice on Comet Hartley 2 (Sunshine et al. 2012). While water ice has been detected on comets, to date, no other ices have been definitively detected via spectroscopy.

Jupiter system

Jupiter has four large moons, discovered 400 years ago by Galileo, and three of these (Europa, Ganymede, and Callisto) were found to have water ice surfaces (Kuiper 1957; Moroz 1965; Johnson and McCord 1971; Pilcher et al. 1972; Fink et al. 1973). Over the years these bodies have been studied using airborne (telescopes on terrestrial aircraft looking up) and ground-based spectroscopy using telescopes (Pollack et al. 1978; Clark 1980; Clark and McCord 1980), by infrared spectroscopy from the *Galileo* spacecraft in orbit around Jupiter (Fig. 11), and from the New Horizons flyby of the Jovian system (Grundy et al. 2007). While no water ice was found on the innermost of the Galilean satellites – Io –sulfur dioxide ice was identified by (Fanale et al. 1979; Hapke 1979; Smythe et al. 1979) on the surface of this moon, the most volcanically active object in the solar system. The vigorous heating that powers Io's volcanoes is the periodic solid-body tidal flexing arising from this moon's orbital eccentricity. An important aspect of Jupiter's satellites is the energetic radiation environment they suffer, far
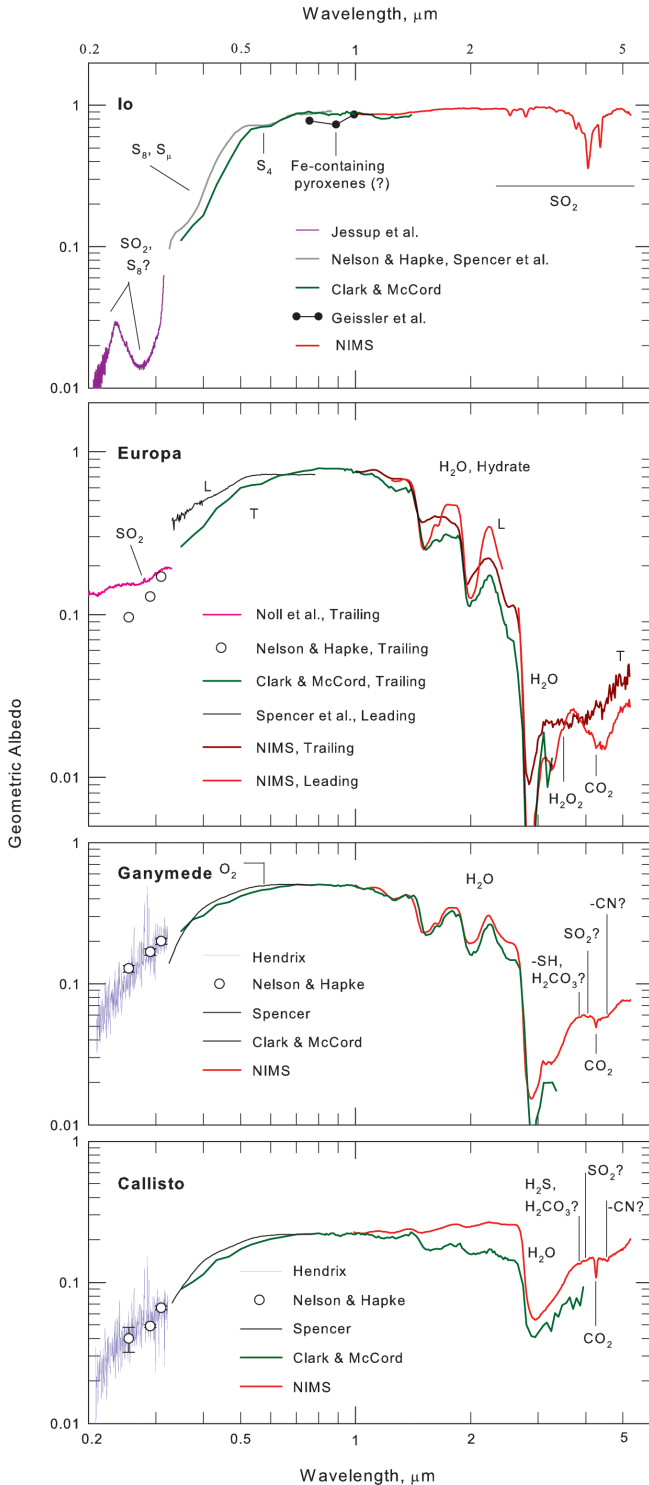
Figure 11. Reflectance spectra of the Galilean Satellites. Geometric albedo spectra derived from ground-based and spaceborne instruments are shown top to bottom as a function of distance from Jupiter. Volcanic Io exhibits a rich infrared spectrum of SO_2 with possible but unidentified polysulfur oxide (PSO) absorption present. The blue edge of sulfur is evident along with a feature at 5 μm due to the S_4 molecule. SO_2 and possibly S_8 absorptions are found in the ultraviolet region. Europa has a leading (L)-trailing (T) side dichotomy so we distinguish these cases. SO_2, polymeric sulfur, and likely S4 are present on the trailing hemisphere along with a hydrate shown at infrared wavelengths by distorted water bands. Nearly pure H_2O is present on Europa's leading side and there is less blue and ultraviolet absorption on that face compared to the sulfurous trailing side. Hydrogen peroxide and carbon dioxide are also apparent in Europa's infrared spectrum. Ganymede has less exposed ice and the geometric albedo is lower due to broad non-ice absorption. Callisto is almost completely covered with dark non-ice compounds and both Callisto and Ganymede show spectral features possibly due to a hydrosulfide or carbonic acid, possibly SO_2, and potentially a CN compound. Trapped O_2 is present on all three of the icy satellites. The Galileo ultraviolet spectrometer data shown for Callisto and Ganymede were kindly provided by A. Hendrix and here normalized to the geometric albedos derived by Nelson and Hapke. Data from Clark and McCord (1980), Nelson et al. (1987), Noll et al. (1995), Spencer et al. (1995), Hendrix et al. (1999), Jessup et al. (2002), Geissler et al. (2004), and Hendrix and Johnson (2008).

more powerful than elsewhere in the solar system. Consequently, the surfaces of these bodies, and particularly that of Io and Europa, will experience modification by radiation chemistry (see review by Johnson et al. 2004).

Gravity data show that Io is a differentiated silicate body with an Fe or Fe + FeS core, whereas the outer three Galilean moons contain significant water ice, with increasing H_2O content as one moves outward from Jupiter. Europa is differentiated and may have an internal structure similar to Io's but with an overlying 100-200 km H_2O mantle that comprises 10% of the satellite's mass. This H_2O cover is thought to consist of a 2-20 km icy crust covering an ocean of up to 100 km thickness. As in the case of Io, tidal flexing provides the heat to sustain a liquid ocean which is likely in contact with the rocky mantle. Ganymede, the largest satellite in the solar system and larger than Mercury, has more water than Europa, contributing to approximately half of the satellite's mass. An outer icy crust and mantle, about 200 km thick, is thought to cover an ocean that is sandwiched between layers of high-pressure ice in different phases. Beneath the H_2O mantle is a differentiated rocky body with a Fe-containing liquid core acting as a magnetic dynamo. Callisto is less differentiated than its sibling satellites, but has about the same relative water content and likely an ocean also, based on Galileo magnetic field data. However, due to their distance from Jupiter, tidal heating is much less efficient for these outer two satellites compared to Io and Europa.

In the following paragraphs we discuss the ice (SO_2 and H_2O) and non-ice surface compositions of Jupiter's Galilean satellites. General reviews can be found in recent publications (Bagenal et al. 2004; Lopes and Spencer 2007; Pappalardo et al. 2009; Dalton et al. 2010; Clark et al. 2013). Io and Europa's surface compositions are reviewed in Carlson et al. *(*2007) and Carlson et al. *(*2009), respectively.

Io. Io is the innermost of the four Galilean satellites and exhibits a young, volcanically active surface that is rapidly resurfaced at an average rate of about one cm per year. The surface is nearly completely covered by sulfur dioxide ice and elemental sulfur, the exceptions being in the hot volcanic areas and fresh lava flows where silicates may be exposed. Gaseous SO_2 is a volcanic effluent, derived from the degassing of hot magma, and is the dominant volcanic gas component, accompanied by minor amounts of SO and S_2 (Zolotov and Fegley 1998, 1999, 2000; Spencer et al. 2000) and other species such as NaCl (Lellouch et al. 2003), identified and mapped through ground-based microwave spectroscopy. SO_2 contributes nearly all of the absorption features in Io's spectra (Fanale et al. 1979; Hapke 1979; Smythe et al. 1979; Schmitt et al. 1994; Nash and Betts 1995; Carlson et al. 1997). The global abundance and grain sizes of the SO_2 particles indicate that optically thick SO_2 deposits of mm-size grains are concentrated in Io's equatorial regions (Carlson et al. 1997; Laver and de Pater 2008; 2009) and confirm earlier measurements of (McEwen 1988), who studied Io's surface using ultraviolet and visible Voyager images. These equatorial deposits are strongly associated with active volcanoes and arise from volcanic venting of gaseous SO_2 into the plumes and atmosphere with subsequent deposition onto colder surfaces as frost. The relatively large grain sizes indicate sublimation and condensation metamorphism for these deposits.

In contrast, fine grained SO_2 frost was found at mid-and high-latitudes (Carlson et al. 1997; Doute et al. 2001; Laver and de Pater 2008, 2009). SO_2 frost sublimates during the day due to relatively high surface temperatures. Although most of it re-condenses locally during the nighttime, SO_2 molecules slowly migrate toward higher latitudes and colder regions (Matson and Nash 1983). The high-latitude SO_2 deposits appear transparent under normal-incidence illumination and therefore are thought to be optically thin (Geissler et al. 2001). They tend to remain as small grains as originally condensed because of the colder environment and rapid radiolytic destruction of the SO_2 grains at higher latitudes (Wong and Johnson 1996). The poles of Io appear red due to the radiolytic destruction of SO_2 and the production of elemental sulfur. The possible condensation of SO_2 during the ~2.5 hour eclipses of Io by Jupiter during each

orbit has long been a subject of interest; see the recent review and time-resolved infrared spectra of Io at eclipse reappearance (Cruikshank et al. 2010a).

Sulfur dioxide is a thermochemical product of hot magmas and its presence is indicative of volcanic conditions. The ratios of SO and S_2 to SO_2 in the volcanic plumes are consistent with high-temperature volcanism in a silicate mantle that is deficient in Fe-metal (Zolotov and Fegley 2000). Being a high-temperature chemical product, SO_2 probably represents a very minor contribution to the satellites total mass. However, since it is a very volatile, it is likely that most of Io's SO_2 is at or near the surface. The solid and gaseous forms of SO_2 are evident in the surficial ices and the overlying sublimational and plume-derived atmosphere, but there is evidence that liquid SO_2 forms a near-surface "aquifer." Scarps and sapping channels provide one line of evidence (McCauley et al. 1979; McEwen et al. 2000; Moore et al. 2001) and uniform topographic infilling of a crater by SO_2 (Lopes et al. 2001) provides further evidence for SO_2 "ground water" (Fig. 12). It has been estimated that the upper 1 km of Io is rich in the volatiles SO_2 and sulfur (McEwen et al. 2000).

Io is intensely irradiated by Jupiter's magnetosphere, forming sulfur trioxide. The signature of SO_3, as well as S_8 and SO_2, may be present in thermal emission spectra of Io (Khanna et al. 1995; Hanel et al. 2003). A related species, disulfur monoxide (S_2O), was investigated by (Baklouti et al. 2008) but interference by strong SO_2 bands precluded its observation. Polysulfur oxides (PSO) may be present on Io and produce a broad absorption in the 4.5-μm region (Baklouti et al. 2008). Ion irradiation can also sputter surface atoms and molecules into an atmosphere around Io and into escape orbits. Neutral and ionized toroidal clouds are formed around Jupiter and provide a source of sulfur, oxygen, sodium, potassium, chlorine, and other possible species to other satellites. This is particularly important for Europa, where the tori strike the trailing hemisphere and provide a source of sulfur and other elements.

Sulfur on Io is emplaced on the surface by volcanic plumes, primarily as S_2, while sulfur volcanism may occur on Io and produce sulfur lava flows. Elemental sulfur can exist in a variety of forms (linear chains, cyclic) and with innumerable lengths. The most stable form is cyclo-octal and some of Io's sulfur is likely in this form, the remaining being polymeric with some tetrasulfur S_4 (Fig. 11, top panel).
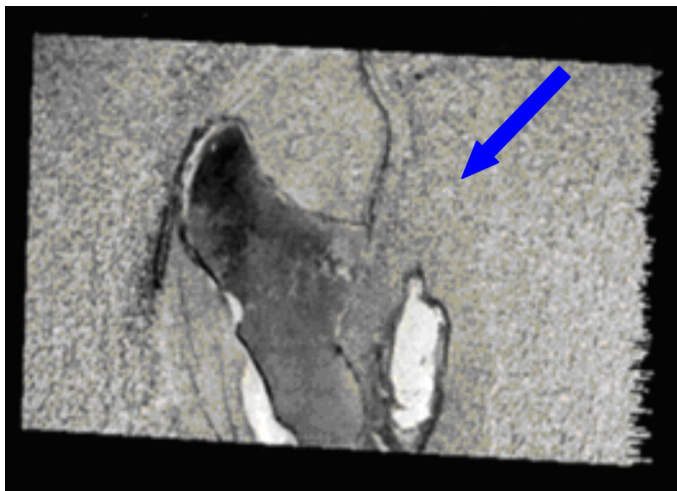

Figure 12. The interior of a volcanic caldera near Chaac (indicated by arrow) on the Galilean moon Io is filled with spectroscopically identified very pure SO_2 that appears white and to be topographically controlled inflows of liquid SO_2.

The high temperatures of Io's volcanoes, up to 1700 K, indicate silicate volcanism but the rapid resurfacing by plume and sublimated SO_2 has precluded definitive identifications of silicates on the surface. Geissler et al. (1999) found a region on Io with an absorption at 0.9 μm and suggested that it was caused by a ferrous iron feature present in Fe-containing magnesian orthopyroxenes. This is a plausible suggestion as such minerals are associated with the most primitive terrestrial rocks and possess a high melting temperature.

Europa. Europa orbits Jupiter at about 1.6 times the distance from Jupiter as Io and is the innermost of the water-ice-containing Galilean satellites. Although it contains less bulk H_2O than Ganymede or Callisto, the surface exhibits much more exposed water ice and hydrate than the other H_2O-icy Galileans due to its greater surface activity, a consequence of tidal heating (the crater age is a mere 50 My as reported by Zahnle et al. 2003). The leading hemisphere of Europa, in the sense of orbital motion, presents the purest ice as determined by infrared spectroscopy which probes the upper sub-millimeter depths of the surficial materials. Both amorphous and crystalline ice are present, with a greater proportion being the amorphous form (Hansen and McCord 2004). The presence of amorphous and crystalline phases are the result of two competing processes—the increase in disorder and amorphization of ice crystals by energetic particle bombardment, and thermally-induced phase transformation of amorphous ice to the lower energy cubic ice form or the even lower energy hexagonal ice phase.

The second major constituent on Europa is a hydrated species, predominant on the trailing side and associated with the dark material that produces Europa's hemispherical color dichotomy—the red, trailing hemisphere and the whiter, leading hemisphere. This icy hydrate is a complex of some molecule X (or groups of molecules) surrounded by hydration shells of water, often in stoichiometric proportions, as $X_n \cdot mH_2O$. One suggested source of this hydrate is a salty subsurface ocean, the X being a salt such as $MgSO_4$, forming hydrates such as epsomite $MgSO_4 \cdot 7H_2O$ and others (McCord et al. 1998b, 1999). A second hypothesis is that radiolysis of exogenic (Iogenic) sulfur implanted on Europa's trailing hemisphere produces hydrated sulfuric acid (Carlson et al. 1999b, 2002, 2005). The associated dark material is thought to be polymeric sulfur (Carlson et al. 1999b) since most salts and acids are colorless in the visible spectral region. The association of hydrate and dark material with geological features on the trailing side implies an endogenic process, either emplacement of material from the subsurface ocean or thermal modification of exogenically-derived material, forming lag deposits. Many hydrated salts exhibit spectral features in the infrared (Dalton et al. 2005; Clark et al. 2007). A linear (areal) mixing model has recently been applied and used to infer composition and variations across Europa's surface (Shirley et al. 2010; Dalton et al. 2012, 2013; Cassidy et al. 2013). The model used many hydrated materials in the fitting, each with a constant grain size, and with areal rather than intimate mixing. Since spectral characteristics are strongly grain-size dependent, the uniqueness of the solutions and identifications must be viewed with caution. Suggestive evidence for the presence of epsomite ($MgSO_4 \cdot 7H_2O$), based on a characteristic 2.07-μm feature, has been found recently by (Brown and Hand 2013). They suggest emplacement of Mg^{2+} and other cations from Europa's ocean as chlorides and subsequent radiolysis (see below) with H_2O ice and exogenic sulfur to produce sulfate salts. However, models with significant salt, like those proposed above, are incompatible with Europa's 3-μm to 5-μm spectrum, which is very dark compared to salts (e.g., see salt spectra in Clark et al. 2007). Future models and interpretations need to include intimate mixtures and the full spectral range of data available for Europa.

The magnetospheric environment at the orbit of Europa is almost as damaging as at Io, and several radiolytic species are observed. As mentioned above, native sulfur exists on the surface and is radiolyzed to the polymeric form and as the red chromophore tetrasulfur (Carlson et al 2009; Hand and Brown 2013). Molecular oxygen is found on Europa (Spencer and Calvin 2002), and is radiolytically formed and trapped in H_2O ice, as is hydrogen peroxide H_2O_2

(Carlson et al. 1999a). SO_2 is observed and is a radiolytic product of sulfate decomposition (Johnson et al. 2004; Carlson et al. 2009; Hendrix et al. 2011). CO_2 is also found (Smythe et al. 1998; Hand et al. 2007; Hansen and McCord 2008) and this ubiquitous molecule could be from endogenic or exogenic sources (see discussions below). These minor species may exist in Europa's near surface as mixed clathrate hydrates (Hand et al. 2006).

Ganymede. Ganymede is also a differentiated body, but is unique because it has an intrinsic magnetic field arising from dynamo motions within a molten iron core. Ganymede and Callisto contain more ice than Europa, but both exhibit darker, less icy surfaces than does Europa. The major source of this dark material is probably the direct infall of meteoritic material and from impact debris ejected from Jupiter's more plentiful but smaller outer satellites. This process should also occur on Europa, but Europa's vigorous current or recent surface activity has diluted and buried the meteoritic material within the ice shell.

Ganymede's surface has roughly equal proportions of amorphous and crystalline ice (Hansen and McCord 2004); the small proportion of amorphous ice compared to Europa is presumably due to the lower incident flux of high-energy magnetospheric radiation and shielding by Ganymede's magnetic field. Bright, icy polar caps are observed on this satellite and the boundary between the icy polar regions and the less icy lower latitudes closely coincides with the transition from open to closed magnetic field lines. This suggests surface brightening by energetic magnetospheric particles streaming in on open field lines and striking Ganymede's polar surfaces. This brightening may be produced by ice grain disruption (Johnson 1997), creating smaller grains and more scattering sites, which decreases the absorption and increases the albedo, or by sputtering and thermal segregation (Khurana et al. 2007).

A hydrate, possibly similar to Europa's, has been identified on Ganymede and suggested to have been formed from $MgSO_4$-rich brine emplaced from the ocean below (McCord et al. 2001). Ganymede once had an active surface but any such emplacement must have occurred in the distant past since the surface age is ~ 2Gy (Zahnle et al. 2003). With subsequent meteoritic infall and gardening, it is unclear how these salt minerals could be present in the high concentrations that were observed. The geological process that erupts material from a 200-km deep ocean is also unclear. A second class of hydrate, associated with dark crater rays, has been identified by Hibbits and Hansen (2007) and found to be similar to C-type asteroid or Callisto non-ice materials. This hydrate may be material from, or modified by, the impactor.

Three water-related radiolytic species are found on Ganymede: molecular oxygen (Spencer et al. 1995; Calvin et al. 1996), ozone (Noll et al. 1996; Hendrix et al. 1999a), and possibly hydrogen peroxide (Hendrix et al. 1999b). Transient, localized SO_2 concentrations have been suggested (Domingue et al. 1998) and spectral information indicates the presence of other species. Since these features are similar to those found in spectra of Callisto, they are described in the following section.

Callisto. Callisto, the outermost icy Galilean satellite, has a bulk composition that is about half H_2O and half rocky silicates. In contrast to the inner three Galilean satellites, Callisto is only partly differentiated, with denser rocky components that slowly settled, or are currently settling, to the center (Schubert et al. 2004). The lack of tidal heating and the low rate of gravitational settling may not provide sufficient energy to cause geological activity on the surface. Callisto has a very old surface, mostly covered with a layer of dark material, presumably from meteoritic infall and outer satellite-derived ejecta material. Both impact cratering and mass wasting have exposed the icy "bedrock" over approximately 10% of this ancient surface, showing the presence of water ice that is predominantly crystalline with grain sizes (diameters) of ~ 200-400 μm (Hansen and McCord 2004). Water molecules tend to segregate by sublimation and condensation on cold, bright ice surfaces, but the dark material also has an H_2O component, probably including adsorbed H_2O. Because the temperatures attained by the dark material are

high (~ 150-160 K), some of these water molecules sublimate during the day and re-condense at night, so thermal segregation is not complete. The radiolysis product O_2 has been observed on Callisto (Spencer and Calvin 2002) and H_2O_2 has been suggested (Hendrix et al. 1999b).

NH$_3$ has not been observed on the surface, but CO_2 is found on the surfaces of Callisto and Ganymede (Carlson et al. 1996; McCord et al. 1997; McCord et al. 1998a; Hibbitts et al. 2000, 2002, 2003) as well as on Europa as noted above. A tenuous CO_2 atmosphere has also been found on Callisto, indicating loss from the surface. The surficial CO_2 is not an ice, based on the spectral position of the absorption feature, and CO_2 ice is too volatile to be stable at Galilean satellite temperatures; instead the molecules appear to be trapped in the dark material. The source of CO_2 could be degassing from the interior (Moore et al. 1999) or an exogenic source or production mechanism. SO_2 has been suggested as a surface component based on ultraviolet (Lane and Domingue 1997; Noll et al. 1997) and infrared spectra (McCord et al. 1997, 1998a; Hibbitts et al. 2000). SO_2 is also quite volatile, and cannot exist as a direct condensate but could be trapped similar to CO_2. Hendrix and Johnson (2008) have questioned the ultraviolet SO_2 identification and interpreted Galileo ultraviolet spectra as absorption by carbonized organics. The radiolysis of organics in ice by energetic electrons as would occur in the Jovian magnetosphere does produce trapped CO_2 (Hand and Carlson 2012). Infrared evidence for the presence of aliphatic hydrocarbons has been suggested by (McCord et al. 1997, 1998a). Two other spectral features have been identified on both Callisto and Ganymede, one at 3.88 μm and thought to be due to a hydrosulfide compound (-SH) (McCord et al. 1997, 1998a) or the CO_2-related compound, carbonic acid (H_2CO_3) (Hage et al. 1998). Another common feature for these two satellites occurs at 4.57 μm and is possibly due to a –CN-containing tholin (McCord et al. 1997, 1998a).

Saturn system

It has long been known that the surfaces of Saturn's rings and major satellites, Mimas, Enceladus, Tethys, Dione, Rhea, Hyperion, Iapetus, and Phoebe are predominantly icy objects (e.g., Fink et al. 1975; Clark et al. 1984, 1986, 2005, 2008a; Roush et al. 1995; Cruikshank et al. 1998a, 2005; Grundy et al. 1999; Owen et al. 2001; Filacchione et al. 2007, 2008; Cuzzi et al. 2009). Whereas the reflectance spectra of these objects (Figs. 13-16) in the visible range indicate that a coloring agent is present on all surfaces, only Phoebe and the dark hemisphere of Iapetus display spectra markedly different from very pure water ice (e.g., Cruikshank et al. 2005; Clark et al. 2005, 2012; Jaumann et al. 2009 and references therein). The relative purity of the ice in Saturn's satellites and rings may be the result of a singular catastrophic event (e.g., Canup 2010; Asphaug and Reufer 2013).

Dark material was first inferred in the Saturn system by J. D. Cassini (1672), and verified by Murphy et al. (1972) and Zellner (1972). The nature of the dark material has been studied by numerous authors, sometimes with conflicting conclusions, including Cruikshank et al. (1983), Vilas et al. (1996), Jarvis et al. (2000), Owen et al. (2001), Buratti et al. (2002), and Villas et al. (2004). The new Cassini VIMS data provide a greater spectral range (0.35 to 5.1 μm in 352 wavelength channels) in reflected solar radiation, with higher precision, and show new absorption features not previously seen in these bodies (e.g., Buratti et al. 2005; Clark et al. 2005, 2008a, 2012; Cruikshank et al. 2007, 2008). These new VIMS observations also spatially resolve the satellite surfaces enabling maps of compounds to be made, leading to additional insights into the nature of the icy satellite surfaces. The spatial resolution of derived maps of materials from VIMS data is variable depending on fly-by distances, and ranges from tens of kilometers per pixel to sub kilometers per pixel.

The Cassini spacecraft entered the Saturn system in 2004, and the Visual and Infrared Mapping Spectrometer (VIMS) began obtaining spatially resolved spectra of Saturn's satellites and rings (Brown et al. 2005a; Figs. 13-16). The VIMS has provided a wealth of spatially
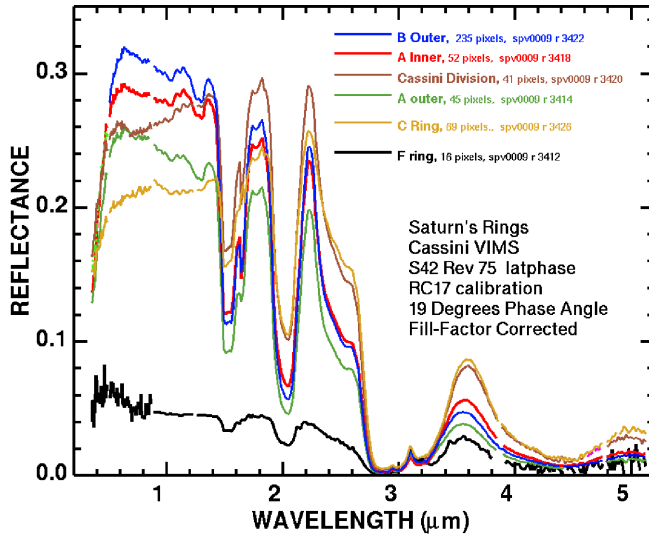
Figure 13. Cassini VIMS reflectance spectra of Saturn's rings corrected for fill factor. The spectra are dominated by absorptions from water ice and an UV absorber. Adapted from data in Cuzzi et al. (2009).
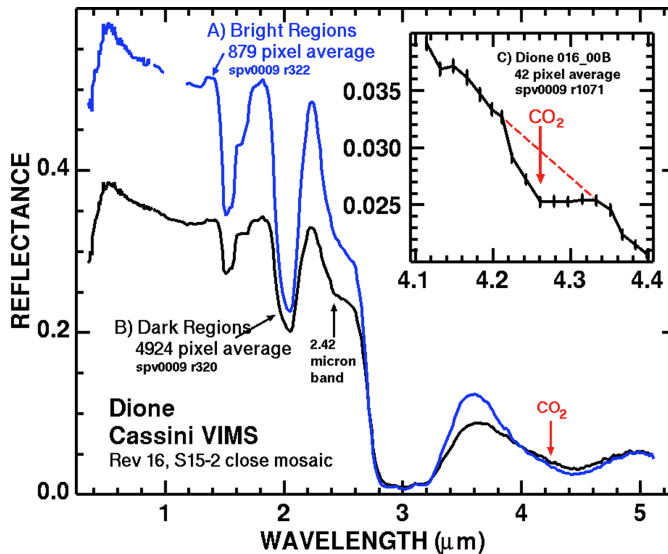

Figure 14. Spectra of bright and dark regions on Saturn's satellite Dione. Inset shows weak CO_2 observed in areas with dark material. From Clark et al. (2008a).

resolved compositional data on the satellites (e.g., Phoebe: Clark et al. 2005; Iapetus: Buratti et al. 2005, Cruikshank et al. 2007, 2008; Enceladus: Brown et al. 2006; Jaumann et al. 2006; Dione: Clark et al. 2008a; Jaumann et al. 2009; Clark et al. 2012) and rings (e.g., Nicholson et al. 2008; Cuzzi et al. 2009). The satellites and rings are dominated by crystalline H_2O ice with trace amounts of CO_2 (Fig. 15) and dark material (e.g., Fig. 14 and Fig. 16 spectra B and C) although it is not clear if the CO_2 is an ice, trapped, or both (Cruikshank et al. 2010b). Trace

Figure 15. CO_2 on icy objects in the Saturn system detected by the absorption near 4.25 μm. No CO_2 has been detected in spectra of the rings. CO_2 absorption appears strongest on satellites with dark material. From Clark et al. (2008a).

Figure 16. Spectra of Iapetus, showing a sequence from regions of dark material (black spectrum) to higher concentrations of water ice (blue). From Clark et al. (2012).

organics and ammonia absorptions are seen in some satellites but again, it is not clear if the absorptions are due to ices or trapped molecules. Unusual colors and spectral shapes of the satellites and rings in the UV to visible are currently explained by a combination of Rayleigh scattering by small particles (ice grains as well as contaminants) and an UV absorber by one of

the contaminants (Clark et al. 2008a,b, 2012; see reviews by Jaumann et al. 2009; Cuzzi et al. 2009; Hendrix et al. 2012).

The surface composition of Titan is still enshrouded in a cloud of mystery despite the initial flood of data from the Cassini spacecraft and the Huygens probe. Although the composition of Titan's atmosphere is known (Coustenis et al. 1999, 2003, 2005, 2006a,b, 2007; Flasar et al. 2005; Teanby et al. 2009 and references therein), with most of the observed gases having been predicted using models of UV photolysis and reactions of atmospheric methane and nitrogen (Yung and DeMore 1999; Vuitton et al. 2008 and references therein), the many less volatile molecules that coat and/or make up the solid surface have yet to be identified. Tholins are the solid end products of photolysis and electron discharge experiments done in terrestrial laboratories with gases common in Titan's atmosphere and are one type of mixture of compounds theorized to exist on Titan (e.g., Sagan et al. 1992; Imanaka et al. 2004; Quirico et al. 2008). Table 1b in Clark et al. (2010a) lists known solid compounds on Titan through 2009, and include benzene (firm), with many tentative or inferred compounds including ices of cyanoacetylene (HC_3N), toluene (C_7H_8), cyanogen (C_2N_2), acetonitrile (CH_3CN), H_2O, CO_2, and NH_3.

The Cassini RADAR has provided the highest spatial resolution images of Titan's surface from Saturn orbit but is a mono-frequency system that provides compositional information only through the dielectric constant of the surface at its operating wavelength of 2.16 cm (Elachi et al. 2005). Only the Descent Imager-Spectral Radiometer, DISR, on the Huygens probe and VIMS from the Cassini Saturn orbiter have the capability to provide combined spectral plus spatial information about the surface (Tomasko et al. 2005; Schroeder and Keller 2008; Sotin et al. 2005; Barnes et al. 2005, 2007, 2008; McCord et al. 2006, 2008; Rodriguez et al. 2006; Brown et al. 2008; Nelson et al. 2009; Soderblom et al. 2009; Clark et al. 2010a). The DISR was limited in wavelength range out to 1.7 μm but obtained very high spatial resolution over a limited area during the descent of the Huygens probe; VIMS measures wavelengths out to 5.1 μm (Fig. 17) and can cover large parts of the surface of Titan, but at much more limited spatial resolution (a few km /pixel are common and a few small areas have been spectrally imaged
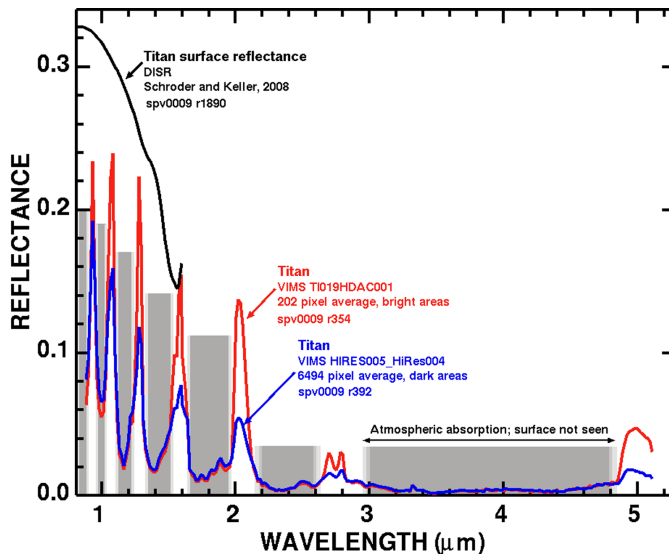

Figure 17. Reflectance spectra of Titan's bright (red line) and dark (blue line) regions. The gray areas in the plot are regions of strong absorption from atmospheric methane through which the surface is not detected. From Clark et al. (2010a).

at sub 300 meters). Terrestrially synthesized tholins do not match the spectral slope in data from the Huygens DISR (Tomasko et al. 2005; Schroeder and Keller 2008) or Cassini VIMS (McCord et al. 2006). The DISR spectra of Titan's surface show a blue spectral slope from 1 to 1.6 μm that is distinctly "un-tholin" like and show what qualitatively appears to be a water-ice absorption, but the complete H_2O feature was not covered by the spectrometer (Tomasko et al. 2005; Schroeder and Keller 2008). Schroeder and Keller concluded the absorption did not match water ice. Also, the 1.25-μm H_2O absorption was not observed even though expected in the models presented by Tomasko et al. (2005) and Schroeder and Keller (2008). *In situ* analyses have detected methane, ethane, and tentatively identified cyanogen, benzene, and carbon dioxide on the surface from the Huygens GCMS (Niemann et al. 2005). Ammonia and hydrogen cyanide were the main pyrolysis products of the aerosols measured by the Huygens *in situ* pyrolysis experiment during its descent (Israel et al. 2005) and those aerosols could rain down to the surface, but pyrolysis products are not necessarily compounds in the aerosols. Higher in Titan's thermosphere, benzene was first detected in the stratosphere by ISO and CIRS (Coustenis et al. 2003, 2007), and the Cassini Ion and Neutral Mass Spectrometer (INMS) instrument has detected high abundances of benzene along with toluene above 900 km (Waite et al. 2007). Toluene is an interesting molecule after benzene because toluene consists of a benzene ring with a methyl functional group, $-CH_3$, replacing one of the hydrogen atoms attached to the benzene ring. Toluene is a possible larger organic molecule that may be compatible with VIMS surface spectra of Titan.

Clark et al. (2010a) presented evidence for surface deposits of solid benzene, (C_6H_6) (Fig. 18), solid and/or liquid ethane, (C_2H_6), or methane (CH_4), and clouds of hydrogen cyanide (HCN) aerosols using diagnostic spectral features in data from the Cassini VIMS. Cyanoacetylene (2-propynenitrile, HC_3N) is indicated in spectra of some bright regions, but the spectral resolution of VIMS is insufficient to make a unique identification although it is a closer match to the feature previously attributed to CO_2. Acetylene (C_2H_2), expected to be more abundant than benzene on Titan according to some models, was not detected. Water ice, if present, must be covered with organic compounds to the depth probed by 1-μm to 5-μm wavelength photons: a few millimeters to centimeters. While many organic compounds have now been detected in the atmosphere and on Titan's surface, we still have only a small spectral database of solid organic compounds measured at Titan temperatures (about 92 K) to compare with spectra of Titan. Spectra of additional compounds are needed, along with higher spatial and
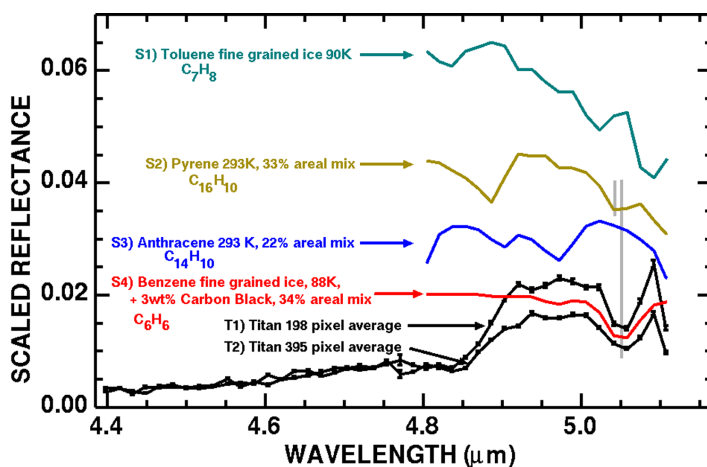

Figure 18. Spectra of Titan showing an absorption attributed to benzene ice. From Clark et al. (2010a).

spectral resolution data of Titan's surface in order to better understand the full compositional range of compounds there.

Saturn's moon Titan has a close analogy to Earth's hydrologic cycle where instead of liquid water, methane and ethane exist as liquids at the surface. Similar to liquid water lakes and rivers on the Earth, Titan has liquid methane and ethane lakes and rivers in a currently active methanologic cycle. These two bodies are unique in the Solar System in that regard.

Uranus system

The Uranus system was investigated by the Voyager II spacecraft in 1986, but that probe had no near-infrared spectral-imaging capability. Accordingly, compositional studies of the Uranian satellites and rings have relied on ground-based telescopic observations, progressing in parallel with advances in infrared instrumentation technology. Prior to the Voyager encounter, low spectral resolution (bandwidths ~2% of the wavelength) circular-variable filter (CVF) spectrophotometry led to detection of broad water ice absorptions at 1.5 and 2 μm on the five major satellites of Uranus: Miranda, Ariel, Umbriel, Titania, and Oberon (Cruikshank 1980; Cruikshank and Brown 1981; Soifer et al. 1981; Brown 1983; Brown and Clark 1984; Brown et al. 1991). Spectrometers based on infrared detector arrays enabled higher quality near-infrared spectra to be obtained (Fig. 19), with spectral bandwidths of around 0.1%, revealing the 1.65-μm water ice band on all five satellites, indicative of cold crystalline H_2O ice (Grundy et al. 1999; Bauer et al. 2002). An apparent dip in Miranda's spectrum near 2.2 μm has been tentatively attributed to ammonia ice (Bauer et al. 2002) but this identification has not yet been confirmed. Repeated observations of the other four satellites have shown no comparable 2.2-μm features, but did reveal the presence of a narrow triplet of CO_2 ice absorptions near 2 μm on Ariel, Umbriel, and Titania, but not Oberon (Grundy et al. 2003, 2006). Interestingly, the strengths of these CO_2 ice absorptions were found to be spatially variable, being strongest on the trailing hemispheres of the satellites, and also on the satellites closer to Uranus (whether or not Miranda fits this pattern remains to be tested). This spatial pattern is consistent with *in situ* production
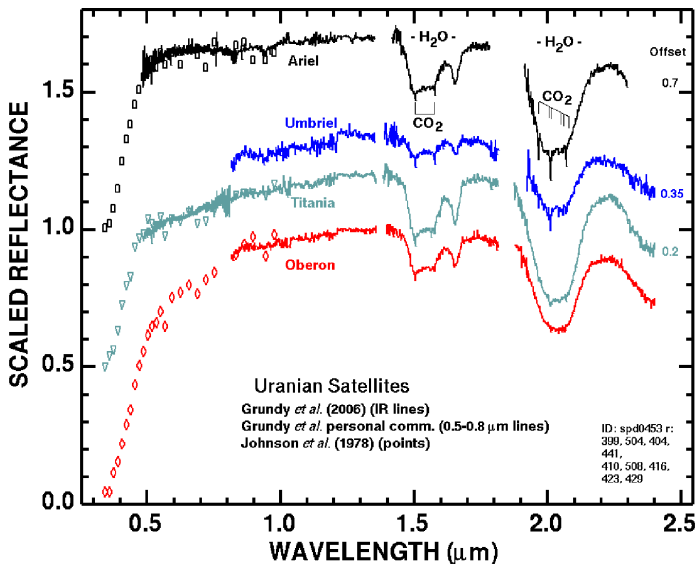

Figure 19. Reflectance spectra of the Uranian satellites showing strong water absorptions and narrow CO_2 absorptions. Note the asymmetric (toward longer wavelengths) 2-μm ice absorption of Oberon indicating the presence of sub-micron ice grains.

of CO_2 from local H_2O plus carbonaceous materials driven by Uranian magnetosphere charged particle radiolysis, balanced by relatively rapid sublimation loss (Grundy et al. 2006). Water ice absorptions were seen to exhibit the opposite pattern, being deepest on the leading hemispheres of Ariel, Umbriel, and Titania (although perhaps not Oberon; Grundy et al. 2006). This pattern of deeper water ice absorptions on leading hemispheres is also seen in the Jovian and Saturnian satellite systems, but the cause remains uncertain. Possibilities include preferential gardening of icy regoliths by impactors impinging on leading hemispheres (Zahnle et al. 2003), and preferential sputtering removal of H_2O ice via magnetospheric charged particle bombardment on trailing hemispheres (e.g., Cheng et al. 1986; Eviatar and Richardson 1986; Pospieszalska and Johnson 1989; Johnson 1990). No ices have been identified to date in spectra of the Uranian rings (e.g., Soifer et al. 1981; Pang and Nicholson 1984; Baines et al. 1998). The low albedos of Uranian satellites and ring particles implies the presence of a darkening agent, which has long been presumed to be carbonaceous in nature, although its precise composition remains unknown.

The Neptune system and beyond

The Neptune system was explored by Voyager 2 in 1989, providing a wealth of physical details. But, as with the Uranus system, almost all compositional information about ices in the Neptune system came from Earth-based observations. Neptune's largest satellite, Triton, provides particularly interesting and complex examples of outer solar system ice geology. Early Triton results came from a series of near-infrared CVF spectrometer observations (~2% spectral resolution) during the 1970s and 1980s, leading to the discovery of methane, nitrogen, and water ice absorptions (Cruikshank and Silvaggio 1979; Apt et al. 1983; Cruikshank and Apt 1984; Cruikshank et al. 1984, 1988, 1989; Rieke et al. 1985).

The advent of array spectrometers with cryogenic optics resulted in much higher quality spectra (Fig. 20), leading to the discovery of CO, CO_2, and C_2H_6 ices (Cruikshank et al. 1993; Bohn et al. 1994; DeMeo et al. 2010). The higher spectral resolution and signal precision enabled by these instruments revealed subtle wavelength shifts in the methane bands consistent
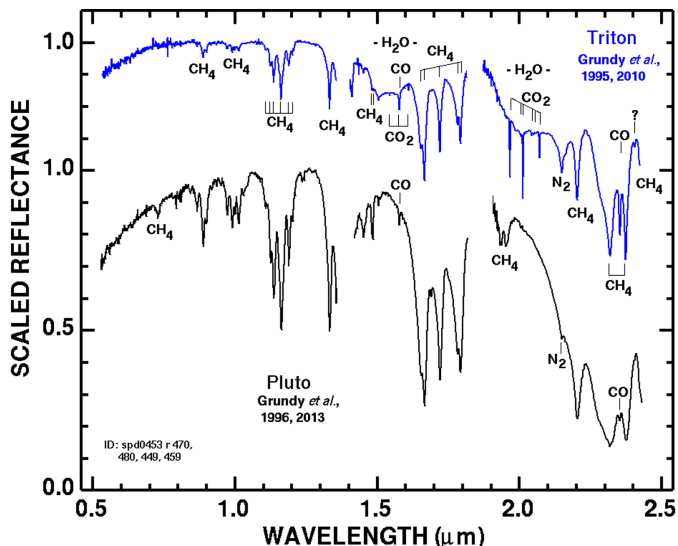

Figure 20. Near infrared spectra of Triton and Pluto are compared in this figure. Features arising from CH_4, CO, CO_2, H_2O, and N_2 are identified.

with the CH_4 molecules being dispersed in nitrogen ice (Cruikshank et al. 1993; Quirico et al. 1999), a situation anticipated from thermodynamic arguments (Lunine and Stephenson 1985). They also revealed the phase of Triton's water ice to be predominantly crystalline (Cruikshank et al. 2000; Grundy and Young 2004).

A picture of Triton emerged of a solar-powered, active world in which volatile N_2, CO, and CH_4 ices sublimate and condense in response to seasonal insolation on a substrate of H_2O and CO_2 ices (which are non-volatile at Triton surface temperatures), leading to an array of bizarre landforms and even jetting of sublimated nitrogen gas out of fissures, with possible aeolian transport of non-volatile H_2O and CO_2 ice dust (e.g., Brown et al. 1990; Hansen and Paige 1992; Stansberry et al. 1996; Grundy et al. 2002). Evidence for short-term changes in the visible wavelength parts of Triton's spectrum reinforced the perception of an active Triton (Hicks and Buratti 2004), as did the paucity of impact craters in Voyager images (Schenk and Zahnle 2007). To explain the large optical path-lengths required by the observed 2.15-μm N_2 absorption band, Triton's N_2 ice could have an unusually compacted texture, perhaps more like a sintered slab than the usual particulate soils encountered on planetary surfaces (e.g., Eluszkiewicz 1991; Grundy and Stansberry 2000). Based on seasonal models, latitudinal heterogeneity in the spatial distribution of Triton's ices is expected, but time-resolved spectroscopy reveals a longitudinal heterogeneity as well (Grundy et al. 2010). The N_2 and CO ices seem to co-occur, and to be much more abundant on Triton's Neptune-facing hemisphere. Despite being mostly dissolved in N_2 ice, Triton's CH_4 shows a very different longitudinal pattern, with its strongest absorption seen on Triton's trailing hemisphere. The H_2O and CO_2 ice absorptions show little or no longitudinal variation, as if they are globally distributed, perhaps as wind-blown dust.

To date, H_2O ice has only been detected on one other body in the Neptune system, the satellite Nereid (Brown et al. 1998, 1999). Little is known beyond photometric colors regarding compositions of Neptune's other satellites and rings (e.g., Dumas et al. 2002).

Objects at Neptune's heliocentric distance and beyond (the transneptunian region, also known as the Kuiper belt) have surface temperatures sufficiently low (<~50 K) for multiple ices to condense on their surfaces. The equilibrium temperature, T_{eq}, of a solid body is a function of both the heliocentric distance (*a*) of the objects and their albedos, (*q*), following the relation T_{eq} = 280 K $((1-q)/a^2)^{1/4}$. For an object at 30 Astronomical Unitts (AU) with an albedo of 0.04 this gives T_{eq} =50.6 K. Larger heliocentric distances, *a*, and/or higher geometric albedos, *q*, lead to even lower temperatures. For objects near condensation thresholds, there is a positive feedback favoring the stability of icy surfaces once the threshold for formation is met. The stability of ices is also a function of surface gravity and the ability of a body to limit atmospheric escape. Schaller and Brown (2007) have calculated the expected stability for CH_4, N_2 and CO ices in outer solar system bodies and find that objects with diameters below 1000-1500 km are not expected to have retained significant amounts of these ices on their surfaces. The handful of larger objects in the Kuiper Belt can retain these materials, and apparently have.

Methane ice was first detected as a solid in the solar system in an infrared spectrum of Pluto (Cruikshank et al. 1976). More recently, solid CH_4 has been identified in the large Kuiper Belt Objects (KBO) Eris (Brown et al. 2005b), Sedna (Barucci et al. 2005), and Makemake (Licandro et al. 2006), as reviewed by de Bergh et al. (2013). The signal-to-noise ratio and wavelength coverage of spectra of small outer solar system objects have steadily improved.

For Pluto in particular, high signal-to-noise ratio spectra show that it shares many spectral features with Triton (Fig. 20) including multiple discrete features of CH_4, although the two clusters of features due to CO_2 ice in Triton's spectrum are absent from Pluto's spectrum. The quality and detail of the spectra allow for detailed analyses comparing band strengths and positions to constrain the detailed physical state of the ices on the surface. As with Triton, the beta N_2 2-0 absorption is interpreted as arising from optical path lengths in beta N_2 ice of the order

of many centimeters, implying unusually coarse particle sizes or perhaps a sintered glaze of N_2 ice, as noted above (e.g., Eluszkiewicz 1991; Grundy and Stansberry 2000). The existence of the ~2.16-μm side band in spectra of both Pluto and Triton has been used to place upper limits on the temperature of N_2 ice on those bodies (Grundy et al. 1993; Tryka et al. 1993, 1994).

Even without directly detecting its absorption bands, it may be possible to infer the presence of N_2 ice from its effect on absorptions from other species. For instance, when CH_4 is dispersed in N_2 ice, the much stronger CH_4 bands are shifted to slightly shorter wavelengths (Quirico and Schmitt 1997a), an effect which has been reported in spectra of Eris and Makemake, in addition to Pluto and Triton. Unfortunately, details of how the distinct CH_4 bands shift depend on the relative concentrations of N_2 and CH_4 are not yet fully understood (e.g., Brunetto et al. 2008; Cornelison et al. 2008), and the uniqueness of N_2 in its ability to shift CH_4 absorption bands has yet to be established. For instance, Tegler et al. (2010) report that dilution of CH_4 in argon ice produces similar shifts.

Pluto shows evidence for time-varying albedo features on its surface (Buie et al. 2010). Seasonal effects are expected to result in redistribution of surface ices over time. Grundy et al. (2013) have recently shown what appears to be seasonal evolution of features on Pluto over a decade of observation. Differing longitudinal variations of CH_4 and N_2 ices suggest that these two ices may be physically segregated on the surface. In contrast, CO and N_2 vary together with longitude, implying they are intimately mixed. Ethane ice has also been reported in spectra of Pluto, notably using bands at 2.27, 2.405, 2.457, and 2.461 μm (DeMeo et al. 2010), where it presumably forms through radiolysis and or photolysis of CH_4 (Moore and Hudson 2003).

Water ice has been detected on numerous Kuiper belt objects and Centaurs, both small and large (e.g., Dotto et al. 2003; Barkume et al. 2008; Guilbert et al. 2009). However, it seems to be absent from some of them. For most of the smaller objects, the bands are fairly shallow, consistent with their low albedos. Systematic changes in albedo and color from the Kuiper belt through the inner solar system could be linked to the sublimation loss of H_2O ice (Grundy 2009; Lamy and Toth 2009). Reports of weak absorptions at 2.2 μm in spectra of Kuiper belt objects have been tentatively attributed to ammonia or ammoniated species (e.g., Delsanti et al. 2010) and an absorption at 2.27 μm in spectra of several objects has been interpreted as resulting from methanol ice (Cruikshank et al. 1998b; Merlin et al. 2012).

The dwarf planet Haumea along with its largest satellite Hi'iaka are noteworthy for their particularly deep water ice bands (e.g., Barkume et al. 2006; Trujillo et al. 2007; Pinilla-Alonso et al. 2009). Several members of the Haumea collisional family also have similar water-rich spectral characteristics, suggesting they could be fragments of the icy mantle of a differentiated target body (Brown et al. 2007; Leinhardt et al. 2010).

A similar catastrophic impact scenario may apply in the Pluto system (Canup 2005, 2011). Unlike Pluto, the largest satellite Charon has a water ice dominated surface (Buie et al. 1987). Additionally, Charon's spectrum shows strong evidence for NH_3 ice (Cook et al. 2007). Charon may represent a sample of Pluto's mantle material which was too small to retain the more volatile CH_4, N_2, and CO ices which mask Pluto's own mantle from view. The compositions of Pluto's small satellites remain unknown.

SUMMARY

Minerals and ices are ubiquitous in the solar system. From the Earth and farther from the Sun, water ice and other more volatile ices are common. As our observational technology has improved, we have found more minerals and other solid compounds in more locations. If water ice in the poles of Mercury can be confirmed, water ice would be found throughout the solar system on every planet and/or their moons with the exception of Venus.

The Earth displays the greatest mineralogic diversity in the Solar System, due to two primary factors. First and foremost, the active volcanism, plate tectonics, and weather in a relatively warm environment provide the conditions for many chemical processes, leading to diverse compositions. Second, because we live on the Earth, we can study it in far greater detail than any other moon or planet.

But as we explore other worlds, we are finding they too have diverse mineralogy. On Mars, for example, it was difficult to prove a case for any clay minerals on the surface as recently as a decade or so ago. But now with orbiting imaging spectrometers with spatial resolutions as low as about 20 m, smaller outcrops are being found to contain diverse mineralogy indicative of a more complex geologic history.

There are outstanding issues. Some small absorptions seen in spectra of outer solar system objects have yet to be identified. For example, possible SO_2 absorptions on the outer three icy Galilean satellites need confirmation. A 2.42-μm absorption seen in spectra of Saturn's satellites, identified as trapped H_2, needs confirmation, and a 5.01-μm absorption seen in spectra of Titan remains unidentified. Some absorptions seen in CRISM spectra of Mars are also still unidentified or poorly understood. This implies a continuing need for improving spectral libraries of reference compounds.

Water ice dominates most icy objects in the outer solar system. But why is the ice so pure in Saturn's rings and most satellites, yet Titan is covered in organics? Similarly, Pluto is covered in organics yet its moon Charon displays a relatively pure water ice surface. What drives most surfaces to show such pure water surfaces with few other ices is unknown. Where are the expected signatures of ammonia or ammonia-water mixtures? If methane is so abundant on Pluto, Triton, Eris, Makemake, and Titan, why is it not abundant on other objects?

Why are some objects very high in albedo with relatively pure ice surfaces while others are very dark (e.g., Phoebe, the two faces of Iapetus, brighter Hyperion, dark Callisto versus brighter Ganymede and Europa)? Some of the answers certainly relate to resurfacing (e.g., Europa and Enceladus), whereas others display ancient heavily cratered surfaces that are still bright (e.g., Rhea) and still other ancient surfaces are dark (e.g., Phoebe). The mechanisms leading to these diverse surface compositions are not completely understood, although there is a trend in the Jupiter and Saturn systems for increasing darkening on moons farther from the planet, implying that dark dust preferentially coats the outer moons, probably from sources external to the system.

How are molecules complexed with one another, as in the case of CO_2 and CH_4 enclathrated in H_2O, and what are the spectroscopic and physical-chemical implications of the processes that lead to complexing?

If water condenses below 135 K, it is expected to be amorphous. Yet the spectra of water ice throughout the solar system is dominated by crystalline ice (where our spectra are of sufficient quality to distinguish between amorphous versus crystalline water ice), with the exception of icy satellites orbiting within Jupiter's inner magnetosphere where intense radiation can destroy the ice crystal structure. Even in the outer solar system beyond Saturn, where temperatures are well below 90 K, observed water ices are at least partially crystalline. Why we do not observe more amorphous ice is a mystery.

Spectroscopy and imaging spectroscopy have played major roles in exploring the solar system, and will continue to do so into the future.

ACKNOWLEDGMENTS

REFERENCES

Anders E, Grevesse N (1989) Abundances of the elements: Meteoritic and solar. Geochim Cosmochim Acta 53:197-214

Apt J, Carleton NP, Mackay CD (1983) Methane on Triton and Pluto: New CCD Spectra. Astrophys J 270:342-350

Asphaug E, Reufer A (2013) Late origin of the Saturn system. Icarus 223:544-565

Bagenal F, Dowling TE, McKinnon WB (eds) (2004) Jupiter. Cambridge University Press, Cambridge

Baines KH, Bellucci G, Bebring JP, Brown RH, Bussoletti E, Capaccioni F, Cerroni R, Clark RN, Coradini A, Cruikshank DP, Drossart P, Formisano V, Jauman R, Langevin Y, Matson DL, McCord TB, Mennella V, Nelson RM, Nicholson PD, Sicardy B, Sotin C, Hansen GB, Aiello JJ, Amici S, the Cassini VIMS team (2000) Detection of sub-micron radiation from the surface of Venus by the Cassini/VIMS. Icarus 148:307-311

Baines KH, Yanamandra-Fisher PA, Lebofsky LA, Momary TW, Golisch W, Kaminski C, Wild WJ (1998) Near-infrared absolute photometric imaging of the Uranian system. Icarus 132:266-284

Baklouti D, Schmitt B, Brissaud O (2008) S_2O, polysulfur oxide and sulfur polymer on Io's surface? Icarus 194:647-659

Bandfield JL, Glotch TD, Christensen PR (2003) Spectroscopic identification of carbonates in the Martian dust. Science 301:1084:1987

Bandfield JL, Hamilton VE, Christensen PR, McSween HY Jr (2004) Identification of quartzofeldspathic materials on Mars. J Geophys Res109:E10009, doi: 10.1029/2004JE002290

Barkume K.M, Brown ME, Schaller EL (2006) Water ice on the satellite of Kuiper belt object 2003 EL61. Astrophys J 640:L87-L89

Barkume KM, Brown ME, Schaller EL (2008) Near-infrared spectra of Centaurs and Kuiper belt objects. Astron J 135:55-67

Barnes JW, Brown RH, Soderblom L, Sotin C, Le Mouélic S, Rodriguez S, Jaumann R, Beyer RA, Buratti BJ, Pitman K, Baines KH, Clark R, Nicholson P (2008) Spectroscopy, Morphometry, and Photoclinometry of Titans Dunefields from Cassini/VIMS. Icarus 195:400-414, doi: 10.1016/j.icarus.2007.12.006

Barnes JW, Brown RH, Turtle EP, McEwen AS, Lorenz RD, Janssen M, Schaller EL, Brown ME, Buratti BJ, Sotin C, Griffith C, Clark R, Perry J, Fussner S, Barbara J, West R, Elachi C, Bouchez AH, Roe HG, Baines KH, Bellucci G, Bibring JP, Capaccioni F, Cerroni P, Combes M, Coradini A, Cruikshank DP, Drossart P, Formisano V, Jaumann R, Langevin Y, Matson DL, McCord TB, Nicholson PD, Sicardy B (2005) A 5-μm bright spot on Titan: Evidence for surface diversity: Science 310:92-94, http://www.sciencemag.org/cgi/content/full/310/5745/92

Barnes JW, Radebaugh J, Brown RH, Wall S, Soderblom L, Lunine J, Burr D, Sotin C, Le Mouélic S, Rodriguez S, Buratti BJ, Clark RN, Baines RN, Jaumann R, Nicholson PD, Kirk RL, Lopes R, Lorenz RD, Mitchell K, Wood CA (2007) Near-infrared spectral mapping of Titan's mountains and channels. J Geophys Res 112:E11006, doi: 10.1029/2007JE002932

Barry P, Shepanski J, Segal C (2001) On-orbit spectral calibration verification of the Hyperion instrument, IGARSS presentation. http://eo1.gsfc.nasa.gov/new/validationReport/Technology/TRW_EO1%20 Papers_Presentations/21.pdf

Barucci MA, Cruikshank DP, Dotto E, Merlin F, Poulet F, Dalle Ore C, Fornasier S, de Bergh C (2005) Is Sedna another Triton? Astron Astrophys 439:L1-L4

Bauer JM, Roush TL, Geballe TR, Meech KJ, Owen TC, Vacca WD, Rayner JT, Jim KTC (2002) The near infrared spectrum of Miranda: Evidence of crystalline water ice. Icarus 158:178-190

Bibring JP, Langevin Y, Mustard JF, Poulet F, Arvidson R, Grendin A, Gondet B, Mangold N, Pinet P, Forget F, Berthe M, Bibring J-P, Gomez C, Jouglet D, Soufflot A, Vincendon M, Combes M, Drossart P, Encrenaz T, Fouchet T, Merchiorri R, Belluci G-C, Altieri F, Formisano V, Capaccioni F, Cerroni P, Coradini A, Fonti S, Korablev O, Kottsov V, Ignatiev N, Moroz V, Titov D, Zasova L, Loiseau D, Doute S, Schmitt B, Sotin C, Hauber E, Hoffmann H, Jaumann R, Keller U, Duxbury T, Neukum G (2006) Global mineralogical and aqueous mars history derived from OMEGA/Mars Express data. Science 312(5772):400-404, doi: 10.1126/science.1122659

Bibring J-P, Langevin Y, Poulet F, Gendrin A, Gondet B, Berthé M, Soufflot A, Drossart P, Combes M, Bellucci G, Moroz V, Mangold N, Schmitt B and the OMEGA team (2004b) Perennial water ice identified in the south polar cap of Mars. Nature 428:627-630

Bibring J-P, Soufflot A, Berthé M, Langevin Y, Gondet B, Drossart P, Bouyé M, Combes M, Puget P, Semery A, Bellucci G, Formisano V, Moroz V, Kottsov V, Bonello G, Erard S, Forni O, Gendrin A, Manaud N, Poulet F, Poulleau G, Encrenaz T, Fouchet T, Melchiori R, Altieri F, Ignatiev N, Titov D, Zasova L, Coradini A, Capacionni F, Cerroni P, Fonti S, Mangold N, Pinet P, Schmitt B, Sotin C, Hauber E, Hoffmann H, Jaumann R, Keller U, Arvidson R, Mustard J, Forget F (2004a) OMEGA: Observatoire pour le Minéralogie, l'Eau, les Glaces et l'Activité´. European Space Agency Special Publication 1240:37-49

Bishop JL, Noe Dobrea EZ, McKeown NK, Parente M, Ehlmann BL, Michalski JR, Milliken RE, Poulet F, Swayze GA, Mustard JF, Murchie SL, Bibring J-P (2008) Phyllosilicate diversity and past aqueous activity revealed at Mawrth Vallis, Mars. Science 321(5890):830-833, doi: 10.1126/science.1159699

Bishop JL, Parente M, Weitz CM, Noe Dobrea EZ, Roach LH, Murchie SL, McGuire PC, McKeown NK, Rossi CM, Brown AJ, Calvin WM, Milliken R, Mustard JF (2009) Mineralogy of Juventae Chasma: Sulfates in light-toned mounds, mafic minerals in the bedrock, and hydrated silica and hydroxylated ferric sulfate on the plateaus. J Geophys Res 114:E00D09, doi: 10.1029/2009JE003352

Bohn RB, Sandford SA, Allamandola LJ, Cruikshank DP (1994) Infrared spectroscopy of Triton and Pluto ice analogs: The case for saturated hydrocarbons. Icarus 111:151-173

Brown ME, Barkume KM, Blake GA, Schaller EL, Rabinowitz DL, Roe HG, Trujillo CA (2007) Methane and ethane on the bright Kuiper belt object 2005 FY9. Astron J 133:284-289

Brown ME, Hand KP (2013) Salts and radiation products on the surface of Europa. Astron J 145:110

Brown ME, Koresko CD, Blake GA (1998) Detection of water ice on Nereid. Astrophys J 508:L175-L176

Brown ME, Trujillo CA, Rabinowitz DL (2005b) Discovery of a planetary-sized object in the scattered Kuiper Belt. Astryphys J 635:L97-L100

Brown RH (1983) The uranian satellites and Hyperion: New spectrophotometry and compositional implications. Icarus 56:414-425

Brown RH, Baines KH, Bellucci G, Bibring JP, Buratti BJ, Bussoletti E, Capaccioni F, Cerroni P, Clark RN, Coradini A, Cruikshank DP, Drossart P, Formisano V, Jaumann R, Langevin Y, Matson DL (2005a) The Cassini visual and infrared mapping spectrometer investigation. Space Sci Rev 115(1-4):111-168

Brown RH, Clark RN (1984) Surface of Miranda: Identification of water ice. Icarus 58:288-292

Brown RH, Clark RN, Buratti BJ, Cruikshank DP, Barnes JW, Mastrapa RME, Bauer J, Newman S, Momary T, Baines KH, Bellucci G, Capaccioni F, Cerroni P, Combes M, Coradini A, Drossart P, Formisano V, Jaumann R, Langevin Y, Matson DL, McCord TB, Nelson RM, Nicholson PD, Sicardy B, Sotin C (2006) Composition and Physical Properties of Enceladus Surface. Science 311:1425-1428

Brown RH, Cruikshank DP, Pendleton Y, Veeder GJ (1999) Water ice on Nereid. Icarus 139:374-378

Brown RH, Johnson TV, Synnott S, Anderson JD, Jacobson RA, Dermott SF, Thomas PC (1991) Physical properties of the Uranian satellites. *In:* Uranus. Bergstralh JT, Miner ED, Matthews MS (eds) University of Arizona Press, Tucson, p 513-527

Brown RH, Kirk RL, Johnson TV, Soderblom LA (1990) Energy sources for Triton's geyser-like plumes. Science 250:431-435

Brown RH, Soderblom LA, Soderblom JM, Clark RN, Jaumann R, Barnes JW, Sotin C, Buratti B, Baines KH, Nicholson PD (2008) The identification of liquid ethane in Titan's Ontario Lacus. Nature 454:607-610

Brunetto R, Caniglia G, Baratta GA, Palumbo ME (2008) Integrated near-infrared band strengths of solid CH4 and its mixtures with N2. Astrophys J 686:1480-1485

Buie MW, Cruikshank DP, Lebofsky LA, Tedesco EF (1987) Water frost on Charon. Nature 329:522-523

Buie MW, Grundy WM, Young EF, Young LA, Stern SA (2010) Pluto and Charon with the Hubble Space Telescope. II. Resolving changes on Pluto's surface and a map for Charon. Astron J 139:1128-1143

Buratti BJ, Cruikshank DP, Brown RH, Clark RN, Bauer JM, Jaumann R, McCord TB, Simonelli DP, Hibbitts CA, Hansen GA, Owen TC, Baines KH, Bellucci G, Bibring JP, Capaccioni F, Cerroni P, Coradini A, Drossart P, Formisano V, Langevin Y, Matson DL, Mennella V, Nelson RM, Nicholson PD, Sicardy B, Sotin C, Roush TL, Soderlund K, Muradyan A (2005) Cassini visual and infrared mapping spectrometer observations of Iapetus: Detection of CO_2. Astrophys J 622:L149-L152

Byrne S, Ingersoll AP (2003) A sublimation model for Martian south polar ice features. Science 299:1051-1053

Calvin WM, Johnson RE, Spencer JR (1996) O_2 on Ganymede: Spectral characteristics and plasma formation mechanisms. Geophys Res Lett 23:673-676

Campins H, Hargrove K, Howell ES, Kelley MS, Licandro J, Mothi-Diniz T, Ziffer J, Fernandez Y, Pinilla-Alonso N (2009) Confirming water ice on the surface of Asteroid 24 Themis. American Astronomical Society, DPS meeting #41, #32.05 *http://adsabs.harvard.edu/abs/2009DPS....41.3205C*

Campins H, Hargrove K, Pillina-Alonso N, Howell ES, Kelley MS, Licandro J, Mothe-Dinez T, Fernandez Y, Ziffer J (2010) Water ice and organics on the surface of the Asteroid 24 Themis. Nature 464:1320-1321

Canup RM (2005) A giant impact origin of Pluto-Charon. Science 307:546-550

Canup RM (2010) Origin of Saturn's rings and inner moons by mass removal from a lost Titan-sized satellite. Nature 468:943-946

Canup RM (2011) On a giant impact origin of Charon, Nix, and Hydra. Astron J 141:35.1-9

Carlson RW, Anderson MS, Johnson RE, Schulman MB, Yavrouian AH (2002) Sulfuric acid production on Europa: The radiolysis of sulfur in water ice. Icarus 157:456-463

Carlson RW, Anderson MS, Johnson RE, Smythe WD, Hendrix AR, Barth CA, Soderblom LA, Hansen GB, McCord TB, Dalton JB, Clark RN, Shirley JH, Ocampo AC, Matson DL (1999a) Hydrogen peroxide on the surface of Europa. Science 283:2062-2064

Carlson RW, Anderson MS, Mehlman R, Johnson RE (2005) Distribution of hydrate on Europa: Further evidence for sulfuric acid hydrate. Icarus 177:461-471

Carlson RW, Baines KH, Encrenaz Th, Taylor FW, D Prossart, LW Kamp, Pollack JB, Lellouch E, Collard AD, Calcutt SB, Grinspoon DH, Weissman PR, Smythe WD, Ocampo AC, Danielson GE, Fanale FP, Johnson TV, Kieffer HH, Matson DL, McCord TB, Soderblom L (1991) Galileo infrared imaging spectroscopy measurements at Venus. Science 253:1541-1548

Carlson RW, Calvin WM, Dalton JB, Hansen GB, Hudson RL, Johnson RE, McCord TB, Moore MH (2009) Europa's Surface Composition. *In:* Europa. Pappalardo RT, McKinnon WB, Khurana KK (eds) Univ. Ariz. Press, Tucson, p 283-327

Carlson RW, Johnson RE, Anderson MS (1999b) Sulfuric acid on Europa and the radiolytic sulfur cycle. Science 286:97-99

Carlson RW, Kargel JS, Doute S, Soderblom LA, Dalton B (2007) Io's surface composition. *In:* Io after Galileo. Lopes RMC, Spencer JR (eds) Springer - Praxis, Chichester, p 193-229

Carlson RW, Smythe W, Baines K, Barbinis E, Becker K, Burns R, Calcutt S, Calvin W, Clark R, Danielson G, Davies A, Drossart P, Encrenaz T, Fanale F, Granahan J, Hansen G, Herrera P, Hibbitts C, Hui J, Irwin P, Johnson T, Kamp L, Kieffer H, Leader F, Lellouch E, LopesGautier R, Matson D, McCord T, Mehlman R, Ocampo A, Orton G, RoosSerote M, Segura M, Shirley J, Soderblom L, Stevenson A, Taylor F, Torson J, Weir A, Weissman P (1996) Near-infrared spectroscopy and spectral mapping of Jupiter and the Galilean satellites: Results from Galileo's initial orbit. Science 274:385-388

Carlson RW, Smythe WD, Lopes Gautier RMC, Davies AG, Kamp LW, Mosher JA, Soderblom LA, Leader FE, Mehlman R, Clark RN, Fanale FP (1997) The distribution of sulfur dioxide and other infrared absorbers on the surface of Io. Geophys Res Lett 24:2479-2482

Cassidy TA, Paranicas CP, Shirley JH, Dalton JB, Teolis BD, Johnson RE, Kamp L, Hendrix AR (2013) Magnetospheric ion sputtering and water ice grain size at Europa. Planet. Space Sci 77:64-73

Cassini GD (1672) Phil. Trans. 12:831. Quoted in Alexander, AFO'D, 1962, *The Planet Saturn*, McMillan, New York, 474

Chapman CR (2004) Space weathering of asteroid surfaces. Annu Rev Earth Planet Sci 32:539-567

Cheng AF, Haff PK, Johnson RE, Lanzerotti LJ (1986) Interactions of magnetospheres with icy satellite surfaces. *In*: Satellites. Burns JA, Matthews MS (eds) Univ. Arizona Press, Tucson, p 403-436

Christensen PR, Anderson DL, Stillman CC, Clark RN, Kieffer HH, Malin MC, Pearl JC, Carpenter JC, Bandera NB, Brown FG, Silverman S (1992) Thermal emission spectrometer experiment: Mars Observer Mission. J Geophys Res 97:7719-7734

Christensen PR, Bandfield JL, Clark RN, Edget KS, Hamilton VE, Hoefen T, Kieffer HH, Kuzmin RO, Lane MD, Malin MC, Morris RV, Pearl JC, Pearson R, Roush TL, Ruff SW, Smith MD (2000) Detection of crystalline hematite mineralization on Mars by the Thermal Emission Spectrometer: Evidence for near-surface water. J Geophys Res 105(E4):9623-9644, doi: 10.1029/1999JE001093

Christensen PR, Bandfield JL, Hamilton VE, Ruff SW, Kieffer HH, Titus TN, Malin MC, Morris RV, Lane MD, Clark RN, Jakosky BM, Mellon MT, Pearl JC, Conrath BJ, Smith MD, Clancy RT, Kuzmin RO, Roush T, Mehall GL, Gorelick N, Bender K, Murray K, Dason S, Greene E, Silverman S, Greenfield M (2001) Mars Global Surveyor Thermal Emission Spectrometer experiment: Investigation description and surface science results. J Geophys Res 106(E10):23823-23871, doi: 10.1029/2000JE001370

Christensen PR, Jakosky BM, Kieffer HH, Malin MC, McSween HY, Nealson K, Mehall GL, Silverman SH, Ferry S, Caplinger M, Ravine M (2004) The Thermal Emission Imaging System (THEMIS) for the Mars 2001 Odyssey mission. Space Sci Rev 110:85-130

Clark RN (1979) Planetary reflectance measurements in the region of planetary thermal emission. Icarus 40:94-103

Clark RN (1980) Ganymede, Europa, Callisto, and Saturn's Rings: Compositional analysis from reflectance spectroscopy. Icarus 44:388-409

Clark RN (1981) Water frost and ice: The near-infrared spectral reflectance 0.65-2.5 μm. J Geophys Res 86: 3087-3096

Clark RN (1999) Spectroscopy of rocks and minerals and principles of spectroscopy. *In:* Manual of Remote Sensing. Volume 3. Rencz AN (ed) John Wiley and Sons, New York, p 3-58

Clark RN (2009) Detection of adsorbed water and hydroxyl on the Moon. Science 326:562-564, doi: 10.1126/science.1178105

Clark RN, Lucey PG (1984) Spectral properties of ice-particulate mixtures and implications for remote sensing I: Intimate mixtures. J Geophys Res 89:6341-6348

Clark RN, McCord TB (1980) The Galilean satellites: new near-infrared spectral reflectance measurements (0.65-2.5 μm) and a 0.325-5 μm summary. Icarus 41:323-329

Clark RN, Brown RH, Owensby PD, Steele A (1984) Saturn's satellites: near-infrared spectrophotometry (0.65-2.5 μm) of the leading and trailing sides and compositional implications. Icarus 58:265-281

Clark RN, Fanale FP, Gaffey MJ (1986) Surface composition of natural satellites. *In:* Satellites. Burns JA, Matthews MS (eds) Univ. of Arizona Press, Tucson, p 437-491

Clark RN, Green RO, Swayze GA, Meeker G, Sutley S, Hoefen TM, Livo KE, Plumlee G, Pavri B, Sarture C, Wilson S, Hageman P, Lamothe P, Vance JS, Boardman J, Brownfield I, Gent C, Morath LC, Taggart J, Theodorakos PM, Adams M (2001) Environmental studies of the World Trade Center area after the September 11, 2001 attack. US Geological Survey Open File Report OFR-01-0429, http://pubs.usgs.gov/of/2001/ofr-01-0429/

Clark RN, Swayze GA, Livo KE, Kokaly RF, King TVV, Dalton JB, Vance JS, Rockwell BW, Hoefen T, McDougal RR (2002) Surface reflectance calibration of terrestrial imaging spectroscopy data: a tutorial using AVIRIS. *In:* Proceedings of the 10th Airborne Earth Science Workshop, JPL Publication 02-1, http://speclab.cr.usgs.gov/PAPERS.calibration.tutorial/

Clark RN, Swayze GA, Livo KE, Kokaly RF, Sutley SJ, Dalton JB, McDougal RR, Gent CA (2003) Imaging spectroscopy: Earth and planetary remote sensing with the USGS Tetracorder and expert systems. J Geophys Res 108(E12):5131, doi: 10.1029/2002JE001847

Clark RN, Brown RH, Jaumann R, Cruikshank DP, Nelson RM, Buratti BJ, McCord TB, Lunine J, Baines KH, Bellucci G, Bibring JP, Capaccioni F, Cerroni P, Coradini A, Formisano F, Langevin Y, Matson DL, Mennella V, Nicholson PD, Sicardy B, Sotin C, Hoefen TM, Curchin JM, Hansen G, Hibbits K, Matz KD (2005) Compositional maps of Saturn's moon Phoebe from imaging spectroscopy. Nature 435(7038):66-69, doi: 10.1038/nature03558

Clark RN, Swayze GA, Hoefen TM, Green RO, Livo KE, Meeker G, Sutley S, Plumlee G, Pavri B, Sarture C, Boardman J, Brownfield I, Morath LC (2006) Environmental mapping of the World Trade Center area with imaging spectroscopy after the September 11, 2001 attack. *In*: Urban Aerosols and Their Impacts: Lessons Learned from the World Trade Center Tragedy. ACS Symposium Series 919. Gaffney J, Marley NA (eds) Oxford University Press, p 66-83, plates 4.1-4.6

Clark RN, Swayze GA, Wise R, Livo E, Hoefen T, Kokaly R, Sutley SJ (2007) USGS digital spectral library splib06a. U.S. Geological Survey, Digital Data Series 231. *http://speclab.cr.usgs.gov/spectral.lib06/*

Clark RN, Curchin JM, Jaumann R, Cruikshank DP, Brown RH, Hoefen TM, Stephan K, Moore JM, Buratti BJ, Baines KH, Nicholson PD, Nelson RM (2008a) Compositional mapping of Saturn's satellite Dione with Cassini VIMS and implications of dark material in the Saturn System. Icarus 193:372-386

Clark RN, Cruikshank DP, Jaumann R, Filacchione G, Nicholson PD, Brown RH, Stephan K, Hedman M, Buratti BJ, Curchin JM, Hoefen TM, Baines KH, Nelson R (2008b) Compositional mapping of Saturn's rings and icy satellites with Cassini VIMS. *In*: Saturn After Cassini-Huygens., London, July, 2008 {abstract}

Clark RN, Curchin JM, Hoefen TM, Swayze GA (2009) Reflectance spectroscopy of organic compounds I: Alkanes. J Geophys Res 114:E03001, doi: 10.1029/2008JE003150

Clark RN, Curchin JM, Barnes JW, Jaumann R, Soderblom L, Cruikshank DP, Lunine J, Stephan K, Hoefen TM, Le Mouelic S, Sotin C, Baines KH, Buratti B, Nicholson P (2010a) Detection and mapping of hydrocarbon deposits on Titan. J Geophys Res 115:E10005, doi: 10.1029/2009JE003369

Clark RN, Swayze GA, Leifer I, Livo KE, Kokaly R, Hoefen T, Lundeen S, Eastwood M, Green RO, Pearson N, Sarture C, McCubbin I, Roberts D, Bradley E, Steele D, Ryan T, Dominguez R, and the Airborne Visible/Infrared Imaging Spectrometer (AVIRIS) Team (2010b) A method for quantitative mapping of thick oil spills using imaging spectroscopy. U.S. Geological Survey Open-File Report 20101167, 51, http://pubs.usgs.gov/of/2010/1167/

Clark RN, Wise RA (2011) Mapping with imaging spectroscopy, Fort Cobb Reservoir watershed, southwestern Oklahoma. *In:* Assessment of conservation practices in the Fort Cobb Reservoir watershed, southwestern Oklahoma. Becker CJ (ed) U.S. Geological Survey Scientific Investigations Report 2010–5257, 23

Clark RN, Cruikshank DP, Jaumann R, Brown RH, Curchin JM, Hoefen TM, Stephan K, Dalle Ore CM, Buratti BJ, Filacchione G, Baines KH, Nicholson PD (2012) The Composition of Iapetus: Mapping Results from Cassini VIMS. Icarus 218:831-860

Clark RN, Carlson R, Grundy W, Noll K (2013) Observed ices in the Solar System. *In*: The Science of Solar System Ices. Astrophysics and Space Science Library Series, Vol. 356. Gudipati MS, Castillo-Rogez J (eds) Springer, p 3-46, doi: 10.1007/978-1-4614-3076-6_1

Colaprete A, Schultz P, Heldmann J, Wooden D, Shirley M, Ennico K, Hermalyn B, Marshall W, Ricco A, Elphic RC, Goldstein D, Summy D, Bart GD, Asphaug E, Korycansky D, Landis D Sollitt L (2010) Detection of Water in the LCROSS Ejecta Plume. Science 330:463-468, doi: 10.1126/science.1186986

Cook JC, Desch SJ, Roush TL, Trujillo CA, Geballe TR (2007) Near-infrared spectroscopy of Charon: Possible evidence for cryovolcanism on Kuiper belt objects. Astrophys J 663:1406-1419

Cornelison DM, Tegler SC, Grundy W, Abernathy M (2008) Near-infrared laboratory spectroscopy of CH_4/ N_2 ice mixtures: Implications for icy dwarf planets. Paper presented at The Science of Solar System Ices (ScSSI): A cross-disciplinary workshop, Oxnard CA, 2008 May 5-8

Coustenis A (2005) Formation and evolution of Titan's atmosphere. Space Sci Rev 116:171-184

Coustenis A, Achterberg R, Conrath B, Jennings D, Marten A, Gautier D, Nixon C, Flasar M, Teanby N, Bezard B, Samuelson RE, Carlson R, Lellouch E, Bjoraker G, Romani P, Taylor FW, Irwin P, Fouchet Th, Hubert A, Orton G, Kunde V, Vinatier S, Mondellini J, Abbas M, Courtin R (2006a) The composition of Titan's stratosphere from Cassini/CIRS mid-infrared spectra. Icarus 189:35-62

Coustenis A, Achterberg R, Conrath B, Jennings D, Marten A, Gautier D, Nixon C, Flasar F, Teanby N, Bezard B, Samuelson R, Carlson R, Lellouch E, Bjoraker G, Romani P, Taylor F, Irwin P, Fouchet T, Hubert A, Orton G, Kunde V, Vinatier S, Mondellini J, Abbas M, Courtin R (2007) The composition of Titan's stratosphere from Cassini/CIRS mid-infrared spectra. Icarus 189:35-62

Coustenis A, Bezard B, Gautier D (1989) Titan's atmosphere from Voyager integrated observations – II. The CH_3D abundance and D/H ration from the 900-1200 cm^{-1} spectral region. Icarus 82:67-80 {NOT USED?}

Coustenis A, Negrão A, Salama A, Schulz B, Lellouch E, Rannou P, Drossart P, Encrenaz T, Schmitt B, Boudon V, Nikitin A (2006b) Titan's 3-μm spectral region from ISO high-resolution spectroscopy. Icarus 180:176-185, doi:10.1016/j.icarus.2005.08.007

Coustenis A, Salama A, Schultz B, Ott S, Lellouch E, Encrenaz T, Gautier D, Feuchtgruber H (2003) Titan's atmosphere from ISO mid-infrared spectroscopy. Icarus 161:383-403

Coustenis A, Schmitt B, Khanna R, Trotta F (1999) Plausible condensates in Titan's stratosphere from Voyager infrared spectra. Planet Space Sci 47:1305-1329

Cruikshank DP (1980) Near infrared studies of the satellites of Saturn and Uranus. Icarus 41:246-258

Cruikshank DP, Apt J (1984) Methane on Triton: Physical state and distribution. Icarus 58:306-311

Cruikshank DP, Bell JF, Gaffey MJ, Brown RH, Howell R, Beerman C, Rognstad M (1983) The Dark Side of Iapetus. Icarus 53:90-104

Cruikshank DP, Brown RH (1981) The Uranian satellites: Water ice on Ariel and Umbriel. Icarus 45:607-611

Cruikshank DP, Brown RH, Calvin W, Roush TL, Bartholomew MJ, (1998a) Ices on the satellites of Jupiter, Saturn, and Uranus. *In*: Solar System Ices. Schmitt B, de Bergh C, Festou M (eds) Kluwer Academic, Dordrecht, p 579-606

Cruikshank DP, Brown RH, Clark RN (1984) Nitrogen on Triton. Icarus 58:293-305

Cruikshank DP, Brown RH, Giver LP, Tokunaga AT (1989) Triton: Do we see the surface? Science 245:283-286

Cruikshank DP, Brown RH, Tokunaga AT, Smith RG, Piscitelli JR (1988) Volatiles on Triton: The infrared spectral evidence, 2.0-2.5 microns. Icarus 74:413-423

Cruikshank DP, Dalton JB, Dalle Ore CM, Bauer J, Stephan K, Filacchione G, Hendrix CJ, Hansen CJ, Coradini A, Cerroni P, Tosi F, Capaccioni F, Jaumann R, Buratti BJ, Clark RN, Brown RH, Nelson RM, McCord TB, Baines KH, Nicholson PD, Sotin C, Meyer AW, Bellucci G, Combes M, Bibring JP, Langevin Y, Sicardy B, Matson DL, Formisano V, Drossart P, Mennella V (2007) Surface composition of Hyperion. Nature 448:54-57, doi: 101038/nature05948

Cruikshank DP, Emery JP, Kornei KA, Bellucci G, d'Aversa E (2010a) Eclipse reappearances of Io: Time-resolved spectroscopy (1.9-4.2 μm). Icarus 205:516-527, doi: 10.1016;j.icarus.2009.05.035

Cruikshank DP, Meyer AW, Brown RH, Clark RN, Jaumann R, Stephan K, Hibbitts CA, Sandford SA, Mastrapa RME, Filacchione G, Dalle Ore CM, Nicholson PD, Buratti BJ, McCord TB, Nelson RM, Dalton JB, Baines KH, Matson DL (2010b) Carbon dioxide on the satellites of Saturn: Results from the Cassini VIMS investigation and revision to the VIMS wavelength scale. Icarus 206:561-572, doi: 10.1016/j.icarus.2009.07.012

Cruikshank DP, Owen TC, Ore CD, Geballe TR, Roush TL, de Bergh C, Sandford SA, Poulet F, Benedix GK, Emery JP (2005) A spectroscopic study of the surfaces of Saturn's large satellites: H_2O ice, tholins, and minor constituents. Icarus 175:268-283

Cruikshank DP, Pilcher CB, Morrison D (1976) Pluto - Evidence for methane frost. Science 194:835-837

Cruikshank DP, Roush TL, Bartholomew MJ, Geballe TR, Pendleton YJ, White SM, Bell III JF, Davies JK, Owen TC, de Bergh C, Tholen DJ, Bernstein MP, Brown RH, Tryka KA, Dalle Ore CM (1998b) The composition of Centaur 5145 Pholus. Icarus 135:389-407

Cruikshank DP, Roush TL, Owen TC, Geballe TR, de Bergh C, Schmitt B, Brown RH, Bartholomew MJ (1993) Ices on the surface of Triton. Science 261:742-745

Cruikshank DP, Schmitt B, Roush TL, Owen TC, Quirico E, Geballe TR, de Bergh C, Bartholomew MJ, Dalle Ore CM, Doute S, Meier R (2000) Water ice on Triton. Icarus 147:309-316

Cruikshank DP, Silvaggio PM (1979) Triton: A satellite with an atmosphere. Astrophys J 233:1016-1020

Cruikshank DP, Wegryn E, Dalle Ore CM, Brown RH, Baines KH, Bibring JP, Buratti BJ, Clark RN, McCord TB, Nicholson PD, Pendleton YJ, Owen TC, Filacchione G, and the VIMS Team (2008) Hydrocarbons on Saturn's Satellites Iapetus and Phoebe. Icarus 193:334-343, doi: 10.1016/j.icarus.2007.04.036

Cull S, Arvidson RE, Mellon MT, Wiseman SJ, Clark RN, Titus TN, Morris RV, McGuire P (2010) Seasonal H_2O and CO_2 ice cycles at the Mars Phoenix landing site: 1. Prelanding CRISM and HiRISE observations. J Geophys Res 115:E00D16, doi: 10.1029/2009JE003340

Cuzzi J, Clark R, Filacchione G, French R, Johnson R, Marouf E, Spilker L (2009) Ring particle composition and size distribution. *In*: Saturn from Cassini/Huygens. Dougherty M, Esposito L, Krimigis S (eds) Springer, p 459-509, doi: 10.1007/978-1-4020-9215-2

Dalton JB, Cassidy T, Paranicas C, Shirley JH, Prockter LM, Kamp LW (2013) Exogenic controls on sulfuric acid hydrate production at Europa. Planet Space Sci 77:45-63

Dalton JB, Cruikshank DP, Stephan K, McCord TB, Coustenis A, Carlson RW, Coradini A (2010) Chemical Composition of Icy Satellite Surfaces. Space Science Review Series 153. Springer

Dalton JB, Prieto-Ballesteros O, Kargel JS, Jamieson CS, Jolivet J, Quinn RC (2005) Spectral comparison of heavily hydrated salts with disrupted terrains on Europa. Icarus 177:472-490

Dalton JB, Shirley JH, Kamp LW (2012) Europa's icy bright plains and dark linea: Exogenic and endogenic contributions to composition and surface properties. J Geophys Res Planets 117:E03003, doi: 10.1029/2011JE0033909

Davies JK, Geballe TR, Hanner MS, Weaver HA, Crovisier J, Bockelée-Morvan D (1997) Thermal infrared spectra of comet Hale-Bopp at heliocentric distances of 4 and 2.9 AU, Earth Moon Planets 78:293-298

de Bergh C, Schaller EL, Brown ME, Brunetto R, Cruikshank DP, Schmitt B (2013) The ices on transneptunian objects and Centaurs. *In:* The Science of Solar System Ices. Astrophysics and Space Science Library Series, Volume 356. Gudipati MS, Castillo-Rogez J (eds) Springer, p. 107-146, doi: 10.1007/978-1-4614-3076-6_1

Delsanti A, Merlin F, Guilbert-Lepoutre A, Bauer J, Yang B, Meech KJ (2010) Methane, ammonia, and their irradiation products at the surface of an intermediate-size KBO? A portrait of Plutino (90482) Orcus. Astron Astrophys 520:A40.1-15

DeMeo FE, Dumas C, de Bergh C, Protopapa S, Cruikshank DP, Geballe TR, Alvarez-Candal A, Merlin F, Barucci MA (2010) A search for ethane on Pluto and Triton. Icarus 208:412-424

Domingue DL, Lane AL, Beyer RA (1998) IUE's detection of tenuous SO2 frost on Ganymede and its rapid time variability. Geophys Res Lett 25:3117-3120

Dotto E, Barucci MA, Boehnhardt H, Romon J, Doressoundiram A, Peixinho N, de Bergh C, Lazzarin M (2003) Searching for water ice on 47171 1999 TC36, 1998 SG35, and 2000 QC243: ESO large program on TNOs and Centaurs. Icarus 162:408-414

Doute S, Schmitt B, Lopes-Gautier R, Carlson R, Soderblom L, Shirley J (2001) Mapping SO_2 frost on Io by the modeling of NIMS hyperspectral images. Icarus 149:107-132

Dumas C, Terrile RJ, Smith BA, Schneider G (2002) Astrometry and near-infrared photometry of Neptune's inner satellites and ring arcs. Astron J 123:1776-1783

Ehlmann BL, Mustard JF, Murchie SL, Bibring JP, Meunier A, Fraeman AA, Langevin Y (2011) Subsurface water and clay mineral formation during the early history of Mars. Nature 479(7371):53-60

Ehlmann BL, Mustard JF, Murchie SL, Poulet F, Bishop JL, Brown AJ, Calvin WM, Clark RN, Des Marais DJ, Milliken RE, Roach LH, Roush TL, Swayze GA, Wray JJ (2008) Orbital identification of carbonate-bearing rocks on Mars. Science 322(5909):1828-1832, doi: 10.1126/science.1164759

Ehlmann BL, Mustard JF, Swayze GA, Clark RN, Bishop JL, Poulet F, Des Marais DJ, Roach LH, Milliken RE, Wray JJ, Barnouin-Jha O, Murchie SL (2009) Identification of hydrated silicate minerals on Mars using MRO-CRISM: Geologic context near Nili Fossae and implications for aqueous alteration. J Geophys Res 114:E00D08, doi: 10.1029/2009JE003339

Elachi C, Wall S, Allison M, Anderson Y, Boehmer R, Callahan P, Encrenaz P, Flamini E, Franceschetti G, Gim Y, Hamilton G, Hensley S, Janssen M, Johnson W, Kelleher K, Kirk R, Lopes R, Lorenz R, Lunine J, Muhleman D, Ostro S, Paganelli F, Picardi G, Posa F, Roth L, Seu R, Shaffer S, Soderblom L, Stiles B, Stofan E, Vetrella S, West R, Wood C, Wye L, Zebker H (2005) Cassini Radar Views the Surface of Titan. Science 308:970-974

Eluszkiewicz J (1991) On the microphysical state of the surface of Triton. J Geophys Res 96:19217-19229

Eviatar A, Richardson JD (1986) Predicted satellite plasma tori in the magnetosphere of Uranus. Astrophys J 300:L99-L102

Fanale FP, Brown RH, Cruikshank DP, Clark RN (1979) Significance of absorption features in Io's IR absorption spectrum. Nature 280:761-763

Farmer CB, Davies DW, Laporte DD (1976) Mars: northern summer ice cap—water vapor observations from Viking 2. Science 194:1339-1341, doi: 10.1126/science.194.4271.1339

Farrand WH, Glotch TD, Rice JW, Hurowitz JA, Swayze GA (2009) Discovery of jarosite within the Mawrth Vallis region of Mars: Implications for the geologic history of the region. Icarus 204(2):478-488

Feldman WC, Lawrence DJ, Elphic RC, Barraclough BL, Maurice S, Genetay I, Binder AB (2000) Polar hydrogen deposits on the Moon. J Geophys Res 105:4175-4195

Feldman WC, Maurice S, Binder AB, Barraclough BL, Elphic RC, Lawrence DL (1998) Fluxes of fast and epithermal neutrons from Lunar Prospector: Evidence for water ice at the lunar poles. Science 281:1496-1500

Feldman WC, Maurice S, Lawrence DJ, Little RC, Lawson SL, Gasnault O, Wiens RC, Barraclough BL, Elphic RC, Prettyman TH, Steinberg JT, Binder AB (2001) Evidence for water ice near the Lunar Poles, J Geophys Res 106:23231-23252

Filacchione G, Capaccioni F, McCord TB, Coradini A, Cerroni P, Bellucci G, Tosi F, D'Aversa E, Formisano V, Brown RH, Baines KH, Bibring JP, Buratti BJ, Clark RN, Combes M, Cruikshank DP, Drossart P, Jaumann R, Langevin Y, Matson DL, Mennella V, Nelson RM, Nicholson PD, Sicardy B, Sotin C, Hansen G, Hibbitts K, Showalter M, Newmann S (2007) Saturn's icy satellites investigated by Cassini VIMS. I. Full-disk properties: 350-5100 nm reflectance spectra and phase curves. Icarus 186:259-290

Filacchione G, Capaccioni F, Tosi F, Cerroni P, McCord TB, Baines KH, Bellucci G, Brown RH, Buratti BJ, Clark RN, Cruikshank DP, Cuzzi JN, Jaumann R, Stephan K, Matson DL, Nelson RM, Nicholson PD (2008) Analysis of the Saturnian icy satellites full-disk spectra by Cassini-VIMS. Saturn After Cassini-Huygens, London, July, 2008 (abstract)

Fink U, Dekkers NH, Larson HP (1973) Infrared spectra of the Galilean satellites of Jupiter. Astrophys J 179:L155-L159

Fink U, Larson HP (1975) Temperature dependence of the water-ice spectrum between 1 and 4 microns: application to Europa, Ganymede, and Saturn's rings. Icarus 24:411-420

Flasar FM, Achterberg RK, Conrath BJ, Gierasch PJ, Kunde VG, Nixon CA, Bjoraker GL, Jennings DE, Romani PN, Simon-Miller AA, Bézard B, Coustenis A, Irwin PGJ, Teanby NA, Brasunas J Pearl JC, Segura ME, Carlson RC, Mamoutkine A, Schinder PJ, Barucci A, Courtin R, Fouchet T, Gautier D, Lellouch E, Marten A, Prangé R, Vinatier S, Strobel DF, Calcutt SB, Read PL, Taylor FW, Bowles N, Samuelson RE, Orton GS, Spilker LJ, Owen TC, Spencer JR, Showalter MR, Ferrari C, Abbas MM, Rauli nF, Edgington S, Ade P, Wishnow EH (2005) Titan's Atmospheric Temperatures, Winds, and Composition. Science 308:975-978

Fleischer M, Mandarino JA (1995) Glossary of Mineral Species 1995. The Mineralogical Record Inc., Tucson

Forget F, Hansen GB, Pollack JB (1995) Low brightness temperatures of Martian polar caps: CO_2 clouds or low surface emissivity? J Geophys Res 100(E10):21219-21234

Geissler P, McEwen A, Phillips C, Keszthelyi L, Spencer J (2004) Surface changes on Io during the Galileo mission. Icarus 169:29-64

Geissler P, McEwen AS, Keszthelyi L, Lopes-Gautier RMC, Granahan J, Simonelli DP (2001) Galileo imaging of SO_2 frosts on Io. J Geophys Res 106:33253-33266

Geissler PE, McEwen AS, Keszthelyi L, Lopes-Gautier R, Granahan J, Simonelli DP (1999) Global color variations on Io. Icarus 140:265-282

Gendrin A, Mangold N, Bibring JP, Langevin Y, Gondet B, Poulet F, Bonello G, Quantin C, Mustard J, Arvidson R, LeMouelic S (2005) Sulfates in Martian Layered Terrains: The OMEGA/Mars Express View. Science 307(5715):1587-1591, doi: 10.1126/science.1109087

Goetz AF, Vane G, Soloman JE, Rock BN (1985) Imaging spectrometry for Earth remote sensing. Science 228:1147-1153

Green RO, Conel JE, Carrere V, Bruegge CJ, Margolis JS, Rast M, Hoover G (1990) Determination of the In-Flight Spectral and Radiometric Characteristics of the Airborne Visible/Infrared Imaging Spectrometer (AVIRIS). *In:* Proceedings of the Second Airborne Visible/Infrared Imaging Spectrometer (AVIRIS) Workshop. JPL Publication 90-54, 15-22

Grundy WM (2009) Is the missing ultra-red material colorless ice? Icarus 199:560-563

Grundy WM, Buie MW, Spencer JR (2002) Spectroscopy of Pluto and Triton at 3-4 microns: Possible evidence for wide distribution of nonvolatile solids. Astron J 124:2273-2278

Grundy WM, Buie MW, Stansberry JA, Spencer JR, Schmitt B (1999) Near-infrared spectra of icy outer solar system surfaces: Remote determination of H_2O ice temperatures. Icarus 142:536-549

Grundy WM, Buratti BJ, Cheng AF, Emery JP, Lunsford A, McKinnon WB, Moore JM, Newman SF, Olkin CB, Reuter DC, Schenk PM, Spencer JR, Stern SA, Throop HB, Weaver HA, the New Horizons team (2007) New Horizons mapping of Europa and Ganymede. Science 318:234-237

Grundy WM, Olkin CB, Young LA, Buie MW, Young EF (2013) Near-infrared spectral monitoring of Pluto's ices: Spatial distribution and secular evolution. Icarus 223:710-721

Grundy WM, Schmitt B (1998) The temperature-dependent near-infrared absorption spectrum of hexagonal H_2O ice. J Geophys Res 103:25809-25822

Grundy WM, Schmitt B, Quirico E (1993) The temperature dependent spectra of alpha and beta nitrogen ice with application to Triton. Icarus 105:254-258

Grundy WM, Stansberry JA (2000) Solar gardening and the seasonal evolution of nitrogen ice on Triton and Pluto. Icarus 148:340-346

Grundy WM, Young LA (2004) Near infrared spectral monitoring of Triton with IRTF/SpeX I: Establishing a baseline. Icarus 172:455-465

Grundy WM, Young LA, Spencer JR, Johnson RE, Young EF, Buie MW (2006) Distributions of H_2O and CO_2 ices on Ariel, Umbriel, Titania, and Oberon from IRTF/SpeX observations. Icarus 184:543-555

Grundy WM, Young LA, Stansberry JA, Buie MW, Olkin CB, Young EF (2010) Near-infrared spectral monitoring of Triton with IRTF/SpeX II: Spatial distribution and evolution of ices. Icarus 205:594-604

Grundy WM, Young LA, Young EF (2003) Discovery of CO_2 ice and leading-trailing spectral asymmetry on the Uranian satellite Ariel. Icarus 162:222-229

Guilbert A, Alvarez-Candal A, Merlin F, Barucci MA, Dumas C, de Bergh C, Delsanti A (2009) ESO-Large Program on TNOs: Near-infrared spectroscopy with SINFONI. Icarus 201:272-283

Hage W, Liedl KR, Hallbrucker A, Mayer E (1998) Carbonic acid in the gas phase and its astrophysical relevance. Science 279:1332-1335

Hand KP, Brown ME (2013) Keck II Observations of hemispherical differences in H_{2O2} on Europa. Astrophys J Lett 766: I.21 (4pp)

Hand KP, Carlson RW (2012) Laboratory spectroscopic analyses of electron irradiated alkanes and alkenes in solar system ices. J Geophys Res 117:E03008

Hand KP, Carlson RW, Chyba CF (2007) Energy, chemical disequilibrium, and geological constraints on Europa. Astrobiology 7:1006-1022

Hand KP, Carlson RW, Cooper JF, Chyba CF (2006) Clathrate hydrates of oxidants in the Europan ice shell. Astrobiology 6:463-482

Hanel RA, Conrath BJ, Jennings DE, Samuelson RE (2003) Exploration of the Solar System by Infrared Remote Sensing. Cambridge Univ. Press, Cambridge

Hansen CJ, Paige DA (1992) A thermal model for the seasonal nitrogen cycle on Triton. Icarus 99:273-288

Hansen GB, McCord TB (2004) Amorphous and crystalline ice on the Galilean satellites: A balance between thermal and radiolytic processes. J Geophys Res 109:E01012, 1-19. doi: 10.1029/2003JE002149

Hansen GB, McCord TB (2008) Widespread CO_2 and other non-ice compounds on the anti-Jovian and trailing sides of Europa from Galileo/NIMS observations. Geophys Res Lett 35:L01202

Hapke B (1979) Io's surface and environs: A magmatic-volatile model. Geophys Res Lett 6:799-802

Hapke B (2001) Space weathering from Mercury to the asteroid belt. J Geophys Res 106:10,039-10,073

Hashimoto GL, Roos-Serote M, Sugita S, Gilmore MS, Kamp LW, Carlson RW, Baines KH (2008) Felsic highland crust on Venus suggested by Galileo Near-Infrared Mapping Spectrometer data. J Geophys Res 113:E00B24, doi: 10.1029/2008JE003134

Hendrix AR, Barth CA, Hord CW (1999a) Ganymede's ozone-like absorber: Observations by the Galileo ultraviolet spectrometer. J Geophys Res 104:14169-14178

Hendrix AR, Barth CA, Stewart AIF, Hord CW, Lane AL (1999b) Hydrogen peroxide on the icy Galilean satellites. Lunar and Planetary Science XXX, Vol. LPI Contribution 964. Lunar and Planetary Institute, Houston (CD-ROM). Abstract # 2043

Hendrix AR, Cassidy TA, Johnson RE, Paranicas C, Carlson RW (2011) Europa's disk-resolved ultraviolet spectra: Relationships with plasma flux and surface terrains. Icarus 212:736-743

Hendrix AR, Domingue D, Noll KS (2012) Ultraviolet properties of planetary ices. *In:* Solar System Ices. Astrophysics and Space Library, Volume 356. Murthy G (ed) Springer, p 73-105

Hendrix AR, Johnson RE (2008) Callisto: New insights from Galileo disk-rsolved UV measurements. Astrophys J 687:706-713

Hibbits CA, Hansen GB (2007) The other non-ice material on Ganymede: Dark ray ejecta (abstract). Bull Am Astron Soc 39:428

Hibbits CA, Pappalardo RT, Hansen GB, MCCord TB (2003) Carbon dioxide on Ganymede. J Geophys Res 108:2-1−2-21, doi: 10:1029/2002JE001956

Hibbitts CA, Klemaszewski JE, McCord TB, Hansen GB, Greeley R (2002) CO_2-rich impact craters on Callisto. J Geophys Res 107:14-1−14-12, 5084. 10.1029/2000JE001412

Hibbitts CA, McCord TB, Hansen GB (2000) The distributions of CO_2 and SO_2 on the surface of Callisto. J Geophys Res 105:22541-22557

Hicks MD, Buratti BJ (2004) The spectral variability of Triton from 1997-2000. Icarus 171:210-218

Hobbs (1975) Ice Physics. Oxford University Press, 856 pages

Hoefen TM, Clark RN, Bandfield JL, Smith MD, Pearl JC, Christensen PR (2003) Discovery of olivine in the Nili Fossae Region of Mars. Science 302(5645):627-630

Hunt GR (1977) Spectral signatures of particulate minerals, in the visible and near-infrared. Geophysics 42:501-513

Imanaka H, Khare BN, Elsila JE, Bakes ELO, McKay CP, Cruikshank DP, Sugita S, Matsui T, Zare RN (2004) Laboratory experiments of Titan tholin formed in cold plasma at various pressures: implications for nitrogen-containing polycyclic aromatic compounds in Titan haze. Icarus 168:344-366

Israel G, Szopa C, Raulin F, Cabane M, Niemann H, Atreya S, Bauer S, Brun JF, Chassefiere E, Coll P, Conde E, Coscia D, Haucehecorne A, Millian P, Nguyen MJ, Owen T, Riedler W, Samuelson R, Siguier JM, Steller M, Sternberg R, Vidal-Madjar C, (2005) Complex organic matter in Titan's atmospheric aerosols from in situ pyrolysis and analysis. Nature 438:796-798

Izenberg NRG, Holsclaw M, Domingue DL, McClintock WE, Klima RL, Blewett DT, Kochte MC, Helbert J, D'Amore M, Sprague AL, Vilas F, Solomon SC (2012) Ultraviolet through near-infrared reflectance variation on Mercury and the search for mineralogical telltales. 43rd Lunar and Planetary Science Conference, 2365, *http://www.lpi.usra.edu/meetings/lpsc2012/pdf/2365.pdf*

James PB, Kieffer HH, Paige DA (1993) The seasonal cycle of carbon dioxide on Mars. *In:* MARS (A93-27852 09-91), University of Arizona Press, p. 934-968

Jarvis KS, Vilas F, Larson SM, Gaffey MJ (2000) Are Hyperion and -Phoebe nlinked to Iapetus? Icarus 146: 125-132

Jaumann R, Clark RN, Nimmo F, Hendrix AR, Buratti BJ, Denk T, Moore JM, Schenk PM, Ostro SJ, Srama R (2009) Icy satellites: geological evolution and surface processes. *In*: Saturn after Cassini/Huygens. Dougherty MK, Esposito LW, Krimigis SM (eds) Springer, p 637-681, doi: 10.1007/978-1-4020-9215-2

Jaumann R, Stephan K, Buratti BJ, Hansen GB, Clark RN, Brown RH, Baines KH, Bellucci G, Coradini A, Cruikshank DP, Griffith CA, Hibbitts CA, McCord TB, Nelson RM, Nicholson PD, Sotin C, Wagner R (2006) Distribution of icy particles across Enceladus' surface as derived from Cassini VIMS measurements. Icarus 193(2008):407419, doi: 10.1016/j.icarus.2007.09.013

Jessup KL, Spencer J, Ballester GE, Yelle R, Roessler F, Howell RR (2002) Spatially resolved UV spectra of Io's Prometheus plume and anti-Jovian hemisphere. Bull Am Astron Soc 34:40.02

Johnson RE (1990) Energetic Charged-Particle Interactions with Atmospheres and Surfaces. Springer-Verlag, New York

Johnson RE (1997) Polar ''caps'' on Ganymede and Io revisited. Icarus 128:469-471

Johnson RE, Carlson RW, Cooper JF, Paranicas C, Moore MH, Wong M (2004) Radiation effects on the surfaces of the Galilean satellites. *In:* Jupiter. Bagenal F, McKinnon W (eds) Cambridge University Press, Cambridge, p 485-512

Johnson RE, Jesser WA (1997) O_2/O_3 microatmospheres in the surface of Ganymede. Astrophys J 480:L79-L82

Johnson TV, McCord TB (1971) Spectral geometric albedo of the Galilean satellites 0.3-2.5 microns. Astrophys J 169:589-593

Khanna RK, Pearl JC, Dahmani R (1995) Infrared-spectra and structure of solid-phases of sulfur- trioxide - Possible identification of solid SO_3 on Io surface. Icarus 15:250-257

Khurana KK, Pappalardo RT, Murphy N, Denk T (2007) The origin of Ganymede's polar caps. Icarus 191:193-202

Kieffer HH, Titus TN (2001) TES mapping of Mars' northern seasonal cap. Icarus 154:162-180

Kieffer S, Chase C Jr., Martin TZ, Miner ED, Palluconi FD (1976) Martian North Pole summer temperatures: dirty water ice. Science 194:1341-1344, doi: 10.1126/science.194.4271.1341

Kokaly RF, Despain DG, Clark RN, Livo KE (2003) Mapping the biology of Yellowstone National Park using imaging spectroscopy. Remote Sens Environ 84:437-456

Kramer GY, Besse S, Dhingra D, Nettles J, Klima R, Garrick-Bethell I, Clark RN, Combe JP, Head III JW, Taylor LA, Pieters CM, Boardman J, McCord TB (2011) The spectral peculiarities of Lunar swirls as seen by the Moon mineralogy mapper. J Geophys Res 116:E00G18, doi: 10.1029/2010JE003729

Kuiper GP (1957) Infrared observations of planets and satellites (abstract). Astron J 62:245

Lamy P, Toth I (2009) The colors of cometary nuclei: Comparison with other primitive bodies of the Solar System and implications for their origin. Icarus 201:674-713

Lane AL, Domingue DL (1997) IUE's view of Callisto: Detection of an SO_2 absorption correlated to possible torus neutral wind alterations. Geophys Res Lett 24:1143-1146

Langevin Y, Poulet F, Bibring JP, Gondet B (2005) Sulfates in the North Polar Region of Mars detected by OMEGA/Mars Express. Science 307:1584-1586

Laver C, de Pater I (2008) Spatially resolved SO2 ice on Io, observed in the near IR. Icarus 195:752-757, doi: 10.1016/j.icarus.2007.12.023

Laver C, de Pater I (2009) The global distribution of sulfur dioxide ice on Io, observed with OSIRIS on the WM Keck telescope. Icarus 201:172-181, doi: 10.1016/j.icarus.2008.12.037

Leinhardt ZM, Marcus RA, Stewart ST (2010) The formation of the collisional family around the dwarf planet Haumea. Astrophys J 714:1789-1799

Lellouch E, Crovisier J, Lim T, Bockelee-Morvan D, Leech K, Hanner MS, Altieri B, Schmitt B, Trotta F, Keller HU (1998) Evidence for water ice and estimate of dust production rate in comet Hale-Bopp at 2.9 AU from the Sun. Astron Astrophys 339:L9-L12

Lellouch E, Paubert G, Moses JI, Schneider NM, Strobel DF (2003) Volcanically emitted sodium chloride as a source for Io's neutral clouds and plasma torus. Nature 421:45-47

Licandro J, Pinilla-Alonso N, Pedani M, Oliva E, Tozzi GP, Grundy WM (2006) The methane ice rich surface of large TNO 2005 FY9: A Pluto-twin in the trans-neptunian belt? Astron Astrophys 445:L35-L38

Lichtenberg KA, Arvidson RE, Morris RV, Murchie SL, Bishop JL, Fernandez Remolar D, Glotch TD, Noe Dobrea E, Mustard JF, Andrews-Hanna J, Roach LH (2010) Stratigraphy of hydrated sulfates in the sedimentary deposits of Aram Chaos, Mars. J Geophys Res 115:E00D17, doi: 10.1029/2009JE003353

Loeffler MJ, Teolis BD, Baragiola RA, (2006) A model study of the thermal evolution of astrophysical ices. Astrophys J 639:L103-L106

Lopes RMC, Kamp LW, Doute S, Smythe WD, Carlson RW, McEwen AS, Geissler PE, Kieffer SW, Leader FE, Davies AG, Barbinis E, Mehlman R, Segura M, Shirley J, Soderblom LA (2001) Io in the near infrared: Near-Infrared Mapping Spectrometer (NIMS) results from the Galileo flybys in 1999 and 2000. J Geophys Res 106:33053-33078

Lopes RMC, Spencer JR (eds) (2007) Io after Galileo. Springer-Praxis, Chichester

Lunine JI, Stevenson DJ (1985) Physical state of volatiles on the surface of Triton. Nature 317:238-240

Martonchik JV, Orton GS (1994) Optical constants of solid and liquid methane. Appl Opt 33:8306-8317

Mastrapa RM, Bernstein MP, Sandford SA, Roush TL, Cruikshank DP, Dalle Ore CM (2008) Optical constants of amorphous and crystalline H_2O-ice in the near infrared from 1.1 to 2.6 μm. Icarus 197:307-320

Mastrapa RM, Grundy WM, Gudipati MS (2013) Observed ices in the Solar System. *In:* The Science of Solar System Ices. Astrophysics and Space Science Library, Volume 356. Gudipati MS Castillo-Rogez J (eds) Springer Science+Business Media, p 371-408, doi: 10.1007/978-1-4614-3076-6_1

Matson DL, Nash DB (1983) Ios atmosphere - Pressure control by regolith cold trapping and surface venting. J Geophys Res 88:4771-4783

McCauley JF, Smith BA, Soderblom LA, (1979) Erosional scarps on Io. Nature 280:736-738

McCord TB, Hansen GB , MatsonDL, Johnson TV, Crowley JK, Fanale FP, Carlson RW, Smythe WD, Martin PD, Hibbitts CA, Granahan JC, Ocampo A (1999) Hydrated salt minerals on Europa's surface from the Galileo near-infrared mapping spectrometer (NIMS) investigation. J Geophys Res 104:11827-11851

McCord TB, Hansen GB, Hibbitts CA (2001) Hydrated salt minerals on Ganymede's surface: Evidence of an ocean below. Science 292:1523-1525

McCord TB, Carlson RW, Smythe WD, Hansen GB, Clark RN, Hibbitts CA, Fanale FP, Granahan JC, Segura M, Matson DL, Johnson TV, Martin PD (1997) Organics and other molecules in the surfaces of Callisto and Ganymede. Science 278:271-275

McCord TB, Hansen GB, Buratti BJ, Clark RN, Cruikshank DP, D'Aversa E, Griffith CA, Baines KH, Brown RH, Dalle Ore CM, Filacchione G, Formisano V, Hibbitts CA, Jaumann R, Lunine JI, Nelson RM, Sotin C, and the Cassini VIMS Team (2006) Composition of Titan's surface from Cassini VIMS. Planet Space Sci 54:1524-1539

McCord TB, Hansen GB, Clark RN, Martin PD, Hibbits CA, Fanale FP, Granahan JC, Segura M, Matson DL, Johnson TV, Carlson RW, Smythe WD, Danielson GE, Team TN (1998a) Non-water-ice constituents in the surface material of the icy Galilean satellites from the Galileo near infrared mapping spectrometer investigation. J Geophys Res 103:8603-8626

McCord TB, Hansen GB, Fanale FP, Carlson RW, Matson DL, Johnson TV, Smythe WD, Crowley JK, Martin PD, Ocampo A, Hibbitts CA, Granahan JC (1998b) Salts on Europa's surface detected by Galileo's Near Infrared Mapping Spectrometer. Science 280:1242-1245

McCord TB, Hayne P, Combe JP, Hansen G, Barnes J, Rodriguez S, Le Mouelic S, Baines K, Buratti B, Sotin C, Nicholson P, Jaumann R, Nelson R, and the Cassini VIMS Team (2008) Titan's surface: Search for spectral diversity and composition using the Cassini VIMS investigation. Icarus 194:212-242

McEwen AS (1988) Global color and albedo variations on Io. Icarus 73:385-426

McEwen AS, Belton MJS, Breneman HH, Fagents SA, Geissler P, Greeley R, Head JW, Hoppa G, Jaeger WL, Johnson TV, Keszthelyi L, Klaasen KP, Lopes-Gautier R, Magee KP, Milazzo MP, Moore JM, Pappalardo RT, Phillips CB, Radebaugh J, Schubert G, Schuster P, Simonelli DP, Sullivan R, Thomas PC, Turtle EP, Williams DA (2000) Galileo at Io: Results from high-resolution imaging. Science 288:1193-1198, doi: 10.1126/science.288.5469.1193

McEwen AS, Eliason EM, Bergstrom JW, Bridges NT, Hansen CJ, Delamere WA, Grant JA, Gulick VC, Herkenhoff KE, Kreszthelyi L, Kirk RL, Mellon MT, Squyres SW, Thomas N, Weitz CM (2007) Mars Reconnaissance Orbiter's High 41934 Resolution Imaging Science Experiment (HiRISE). J Geophys Res 935:E05S02, doi: 10.1029/2005JE002605

McGuire PC, Wolff MJ, Smith MD, Arvidson RE, Murchie SL, Clancy RT, Roush TL, Cull SC, Lichtenberg KA, Wiseman SM, Green RO, Martin TZ, Milliken RE, Cavender PJ, Humm DC, Seelos FP, Seelos KD, Taylor HW, Ehlmann BL, Mustard JF, Pelkey SM, Titus TN, Hash CD, Malaret ER, (2008) MRO/CRISM retrieval of surface lambert albedos for multispectral mapping of Mars with DISORT-based radiative transfer modeling: Phase 1 – Using Historical Climatology for temperatures, aerosol optical depths, and atmospheric pressure. IEEE Trans Geosci Remote Sens 46(12):4020-4040

Merlin F, Quirico E, Barucci MA, de Bergh C (2012) Methanol ice on the surface of minor bodies in the solar system. Astron Astrophys 544:A20, doi: 10.1051/0004-6361/201219181

Milliken RE, Grotzinger JP, Thomson BJ (2010) Paleoclimate of Mars as captured by the stratigraphic record in Gale Crater. Geophys Res Lett 37:L04201, doi: 1029/2009GL041870

Milliken RE, Swayze GA, Arvidson RE, Bishop JL, Clark RN, Ehlmann BL, Green RO, Grotzinger JP, Morris RV, Murchie SL, Mustard JF, Weitz C (2008) Opaline silica in young deposits on Mars. Geology 36(11):847-850

Moore JM, Asphaug E, Morrison D, Spencer JR, Chapman CR, Bierhaus B, Sullivan RJ, Chuang FC, Klemaszewski JE, Greeley R, Bender KC, Geissler PE, Helfenstein P, Pilcher CB (1999) Mass movement and landform degradation on the icy Galilean satellites: Results of the Galileo nominal mission. Icarus 140:294-312

Moore JM, Sullivan RJ, Chuang FC, Head JW, III, McEwen AS, Milazzo MP, Nixon B E, Pappalardo RT, Schenk PM, Turtle EP (2001) Landform degradation and slope processes on Io: The Galileo view. J Geophys Res 106:33223-33240, doi: 10.1029/2000je001375

Moore MH, Hudson RL (2003) Infrared study of ion-irradiated N_2-dominated ices relevant to Triton and Pluto: Formation of HCN and HNC. Icarus 161:486-500

Moroz VI (1965) Infrared spectrophotometry of the Moon and the Galilean satellites of Jupiter. Sov Astron 9:999-1006

Müller N, Helbert J, Hashimoto G, Tsang CCC, Piccioni G, Drossart P and Venus Express/VIRTIS Team (2008) Venus surface thermal emission at one micrometer in VIRTIS imaging observations - evidence for variation of crust and mantle differentiation conditions. J Geophys Res 113:E00B17, doi: 10.1029/2008JE003118

Murchie S, Arvidson R, Bedini P, Beisser K, Bibring JP, Bishop J, Boldt J, Cavender P, Choo T, Clancy RT, Darlington EH, Des Marais D, Espiritu R, Fort D, Green R, Guinness E, Hayes J, Hash C, Heffernan K, Hemmler J, Heyler G, Humm D, Hutcheson J, Izenberg N, Lee R, Lees J, Lohr D, Malaret E, Martin T, McGovern JA, McGuire P, Morris R, Mustard J, Pelkey S, Rhodes E, Robinson, M, Roush T, Schaefer E, Seagrave G, Seelos F, Silverglate P, Slavney S, Smith M, Shyong W-J, Strohbehn K, Taylor H, Thompson P, Tossman B, Wirzburger M, Wolff M (2007) Compact Reconnaissance Imaging Spectrometer for Mars (CRISM) on Mars Reconnaissance Orbiter (MRO). J Geophys Res 112:EO5S03, doi: 10.1029/2006JE002682

Murchie SL, Mustard JF, Ehlmann BL, Milliken RE, Bishop JL, McKeown NK, Noe Dobrea EZ, Seelos FP, Buczkowski DL, Wiseman SM, Arvidson RE, Wray JJ, Swayze G, Clark RN, Des Marais DJ, McEwen AS, Bibring J-P (2009) A synthesis of Martian aqueous mineralogy after 1 Mars year of observations from the Mars Reconnaissance Orbiter. J Geophys Res 114:E00D06, doi: 10.1029/2009JE003342

Murphy RE, Cruikshank DP, Morrison D (1972) Radii, albedos, and 20-micron brightness temperatures of Iapetus and Rhea. Astrophys J Lett 177:L93-L96

Mustard JF, Murchie SL, Pelkey SM, Ehlmann BL, Milliken RE, Grant JA, Bibring J-P, Poulet F, Bishop J, Noe Dobrea E, Roach L, Seelos F, Arvidson RE, Wiseman S, Green R, Hash C, Humm D, Malaret E, McGovern JA, Seelos K, Clancy T, Clark R, Des Marais D, Izenberg N, Knudson A, Langevin Y, Martin T, McGuire P, Morris R, Robinson M, Roush T, Smith M, Swayze G, Taylor H, Titus T, and Wolff M (2008) Hydrated silicate minerals on Mars observed by the Mars Reconnaissance Orbiter CRISM instrument. Nature 454:305-309. doi: 10.1038/nature07097

Mustard JF, Poulet F, Gendrin A, Bibring J-P, Langevin Y, Gondet B, Mangold N, Bellucci G, Altieri F (2005) Olivine and pyroxene diversity in the crust of Mars. Science 307(5715):1594-1597, doi: 10.1126/science.1109098

Nash DB, Betts BH (1998) Ices on Io - composition and texture. *In:* Solar System Ices. Schmitt B, de Bergh C, Festou M (eds) Kluwer, Dordrecht, p 607-638

Nelson RM, Kamp LW, Matson DL, Irwin PGJ, Baines KH, Boryta MD, Leader FE, Jaumann R, Smythe WD, Sotin C, Clark RN, Cruikshank DP, Drossart P, Pearl JC, Hapke BW, Lunine J, Combes M, Bellucci G, Bibring JP, Capaccioni F, Cerroni P, Coradini A, Formisano V, Filacchione G, Langevin RY, McCord TB, Mennella V, Nicholson PD, Sicardy B (2009) Saturn's Titan: Surface change, ammonia, and implications for atmospheric and tectonic activity. Icarus 199:429-441

Nelson RM, Lane AL, Matson DL, Veeder GJ, Buratti BJ, Tedesco EF (1987) Spectral geometric albedos of the Galilean satellites from 0.24 to 0.34 micrometers: Observations with the International Ultraviolet Explorer. Icarus. 72:358-380

Nicholson PD, Hedman MM, Clark RN, Showalter MR, Cruikshank DP, Cuzzi JN, Filacchione G, Capaccioni F, Cerroni P, Hansen GB, Sicardy B, Drossart P, Brown RH, Buratti BJ, Baines KH Coradini A (2008) A close look at Saturn's rings with Cassini VIMS. Icarus 193:182-212, doi: 10.1016/j.icarus.2007.08.036

Niemann HB, Atreya S, Bauer S, Carignan G, Demick J, Frost R, Gautier D, Haberman J, Harpold D, Hunten D, Israel G, Lunine J, Kasprzak W, Owen T, Paulkovich M, Raulin F, Raaen E, Way S (2005) The abundance of constituents of Titan's atmosphere from the GCMS instrument on the Huygens probe. Nature 438:779-784

Noe Dobrea EZ, Bishop JL, McKeown NK, Fu R, Rossi CM, Michalski JR, Heinlein C, Hanus V, Poulet F, Mustard JF, Murchie S, McEwen S, Swayze G, Bibring J-P, Malaret E, Hash C (2010) Mineralogy and stratigraphy of phyllosilicate-bearing and dark mantling units in the greater Mawrth Vallis/west Arabia Terra area: Constraints on geological origin. J Geophys Res 115:E00D19, doi: 10.1029/2009JE003351

Noll KS, Johnson RE, Lane AL, Domingue DL, Weaver HA (1996) Detection of ozone on Ganymede. Science 273:341-343

Noll KS, Johnson RE, McGrath MA, Caldwell JJ (1997) Detection of SO_2 on Callisto with the Hubble Space Telescope. Geophys Res Lett 24:1139-1142

Noll KS, Weaver HA, Gonnella AM, (1995) The albedo spectrum of Europa from 2200 angstrom to 3300 angstrom. J Geophys Res Planets 100:19057-19059

Owen TC, Cruikshank DP, Dalle Ore CM, Geballe TR, Roush TL, de Bergh C, Pendleton YJ, Khare BN (2001) Decoding the domino: The dark side of Iapetus. Icarus 149:160-172

Paige DA, Siegler MA, Zhang JA, Hayne PO, Foote EJ, Bennett KA, Vasavada AR, Greenhagen BT, Schofield JT, McCleese DJ, Foote MC, DeJong E, Bills BG, Hartford W, Murray BC, Allen CC, Snook K, Soderblom LA, Calcutt S, Taylor FW, Bowles NE, Bandfield JL, Elphic R, Ghent R, Glotch TD, Wyatt MB, Lucey PG (2010) Diviner Lunar Radiometer Observations of Cold Traps in the Moons South Polar Region. Science 330:479-482, doi: 10.1126/science.1187726

Painter TH, Dozier J, Roberts DA, Davis RE, Green RO (2003) Retrieval of subpixel snow-covered area and grain size from imaging spectrometer data. Remote Sens Environ 85:64-77, doi: 10.1016/S0034-4257(02)00187-6

Pang KD, Nicholson PD (1984) Composition and size of Uranian ring particles. Lunar Planetary Science Conference XV, 627-628 (abstract)

Pappalardo RT, McKinnon WB, Khurana K (eds) (2009) EUROPA. Univ. of Ariz. Press, Tucson

Parente M (2008) A new approach to denoising CRISM images. Lunar Planetary Science Conference XXXIX, 2528.pdf (abstract)

Pieters CM, Besse S, Boardman J, Buratti B, Cheek L, Clark RN, Combe JP, Dhingra D, Goswami JN, Green R, Head JW, Isaacson P, Klima R, Kramer G, Lundeen S, Malaret E, McCord T, Mustard J, Nettles J, Petro N, Runyon C, Staid M, Sunshine J. Taylor LA, Thaisen K, Tompkins S, Whitten J (2011) Mg-Spinel Lithology: A New Rock-type on the Lunar Farside. J Geophys Res 116:E00G08, doi: 10.1029/2010JE003727

Pieters CM, Englert PA (1993) Remote geochemical Analysis: Elemental and Mineralogical Composition, Cambridge Univ. Press, New York

Pieters CM, Goswami JN, Clark RN, Annadurai M, Boardman J, Buratti B, Combe JP, Dyar MD, Green R, Head JW, Hibbitts C, Hicks M, Isaacson P, Klima R, Kramer G, Kumar S, Livo E, Lundeen S, Malaret E, McCord T, Mustard J, Nettles J, Petro N, Runyon C, Staid M, Sunshine J, Taylor LA, Tompkins S, Varanasi P (2009) Character and Spatial Distribution of OH/H_2O on the Surface of the Moon seen by M3 on Chandrayaan-1. Science 326:568-572, doi: 10.1126/science.1178658

Pilcher CB, Ridgeway ST, McCord TB (1972) Galilean satellites: Identification of water frost. Science 178:1087-1089

Pinilla-Alonso N, Brunetto R, Licandro J, Gil-Hutton R, Roush TL, Strazzulla G (2009) The surface of (136108) Haumea (2003 EL61), the largest carbon-depleted object in the trans-Neptunian belt. Astron Astrophys 496:547-556

Pollack JB, Witteborn FC, Erickson EF, Strecker DW, Baldwin BJ, Bunch TE, (1978) Near-infrared spectra of the Galilean satellites: Observations and compositional implications. Icarus 36:271-303

Pospieszalska MK, Johnson RE (1989) Magnetospheric ion bombardment profiles of satellites: Europa and Dione. Icarus 78:1-13

Poulet F, Bibring J-P, Mustard JF, Gendrin A, Mangold N, Langevin Y, Arvidson, RE, Gondet B, and Gomez C (2005) Phyllosilicates on Mars and implications for early Martian climate. Nature 438:623-627, doi: 10.1038/nature04274

Quirico E, Doute S, Schmitt B, de Bergh C, Cruikshank DP, Owen TC, Geballe TR, Roush TL (1999) Composition, physical state, and distribution of ices at the surface of Triton. Icarus 139:159-178

Quirico E, Schmitt B (1997a) Near-infrared spectroscopy of simple hydrocarbons and carbon oxides diluted in solid N_2 and as pure ices: Implications for Triton and Pluto. Icarus 127:354-378

Quirico E, Schmitt B (1997b) A spectroscopic study of CO diluted in N_2 ice: Applications for Triton and Pluto. Icarus 128:181-188

Quirico E, Montagnac G, Lees V, McMillan PF, Szopa C, Cernogora G, Rouzaud JN, Simon P, Bernard JM, Coll P, Fray N, Minard RD, Raulin F, Reynard B, Schmitt B (2008) New experimental constraints on the composition and structure of tholins. Icarus 198:218-231

Ramaprasad KR, Caldwell J, McClure DS (1978) The vibrational overtone spectrum of liquid methane in the visible and near infrared: Applications to planetary studies. Icarus 35:400-409

Rieke GH, Lebofsky LA, Lebofsky MJ (1985) A search for nitrogen on Triton. Icarus 64:153-155

Riner MA, Lucey PG (2012) Intense Space Weathering On Mercury: Are There Any Surface Exposures Of Immature Material?, 43rd Lunar and Planetary Science Conference, 2866. *http://www.lpi.usra.edu/meetings/lpsc2012/pdf/2866.pdf*

Rivkin AS, Emery JP (2008) Water Ice on 24 Themis? Asteroids, Comets, Meteors (abstract), *http://www.lpi.usra.edu/meetings/acm2008/pdf/8099.pdf*

Rivkin AS, Emery JP (2010) Detection of ice and organics on an asteriodal surface. Nature 464:1322-1323

Rodriguez S, Le Mouélic S, Sotin C, Clenet H, Clark R, Buratti B, Brown R, McCord T, Nicholson P, Baines K, and the VIMS Science Team (2006), Cassini/VIMS hyperspectral observations of the HUYGENS landing site on Titan. Planet Space Sci 54:1510-1523

Roush TL, Cruikshank DP, Owen TC (1995) Surface ices in the outer solar system. *In:* Volatiles in the Earth and Solar System. AIP Conference Proceedings 341. Farley KA (eds) Am Inst Phys, New York, p 143-153

Ruff SW (2004) Spectral evidence for zeolite in the dust on Mars. Icarus 168(1):1310-143

Sagan C, Thompson WR, Khare B (1992) Titan: A laboratory for pre-biological organic chemistry. Acc Chem Res 25:286-292

Sanford and Allamandola (1993) The condensation and vaporization behavior of ices containing SO_2, H_2S, and CO_2: implications for Io. Icarus 106:478-88

Schaller EL, Brown ME (2007) Volatile loss and retention on Kuiper belt objects. Astrophys J 659:L61-L64

Schenk PM, Zahnle K (2007) On the negligible surface age of Triton. Icarus 192:135-149

Schmitt B, de Bergh C, Festou M (eds) (1998a) Solar System Ices. Kluwer, Dordrecht

Schmitt B, de Bergh C, Lellouch E, Maillard JP, Barbe A, Doute S (1994) Identification of three absorption bands in the 2-mm spectrum of Io. Icarus 111:79-105

Schmitt B, Quirica E, Trotta F, Grundy WM (1998b) Optical properties of ices from the UV to infrared. *In:* Solar System Ices. Schmitt B, DeBergh C, Festou M (eds) Kluwer, Dordrecht, p 199-240

Schroder SE, Keller HU (2008) The reflectance spectrum of Titan's surface at the Huygens landing site determined by the descent imager/spectral radiometer. Planet Space Sci 56:753-769

Schubert G, Anderson JD, Spohn T, McKinnon WB (2004) Interior composition, structure, and dynamics of the Galilean satellites. *In:* Jupiter: The Atmosphere, Satellites, and Magnetosphere. Bagenal F, Dowling TE, McKinnon W (eds) Cambridge Univ. Press, Cambridge, p. 281-306

Scott (1976) Solid and liquid nitrogen. Phys Rep 27:89-157

Shapiro MM, Gush HP (1966) The collision-induced fundamental and first overtone bands of oxygen and nitrogen. Can J Phys 44:949-963

Sheng DT, Ewing GE (1971) Collision induced infrared absorption of gaseous nitrogen at low temperatures. J Chem Phys 55:5425-5430

Shirley JH, Dalton JB, Prockter LM, Kamp LW (2010) Europa's ridged plains and smooth low albedo plains: Distinctive compositions and compositional gradients at the leading side-trailing side boundary. Icarus 210:358-384

Smythe WD, Carlson RW, Ocampo A, Matson D, Johnson TV, McCord TB, Hansen GE, Soderblom LA, Clark RN, (1998) Absorption bands in the spectrum of Europa detected by the Galileo NIMS instrument. XXIX Lunar and Planetary Science Conference, Vol. CD. Lunar and Planetary Institute, Houston, Texas

Smythe WD, Nelson RM, Nash DB (1979) Spectral evidence for SO_2 frost or adsorbate on Io's surface. Nature 280:766

Soderblom LA, Barnes JW, Brown RH, Clark RN, Janssen MA, McCord TB, Niemann HB, Tomasko MG (2009) Composition of Titan's Surface. *In:* Titan from Cassini-Huygens. Brown RH, Lebreton JP, Waite JH (eds) Springer, p 141-175, doi: 10.1007/978-1-4020-9215-2

Soifer BT, Neugebauer G, Matthews K (1981) Near-infrared photometry of the satellites and rings of Uranus. Icarus 45:612-617

Sotin C, Jaumann R, Buratti BJ, Brown RH, Clark RN, Soderblom LA, Baines KH, Bellucci G, Bibring JP, Capaccioni F, Cerroni P, Combes M, Coradini A, Cruikshank DP, Drossart P, Formisano V, Langevin Y, Matson DL, McCord TB, Nelson RM, Nicholson PD, Sicardy B, LeMouelic S, Rodriguez S, Stephan K, Scholz CK (2005) Release of volatiles from a possible cryovolcano from near-infrared imaging of Titan. Nature 435:786-789, doi: 10.1038nature03596

Spencer JR, Calvin WM (2002) Condensed O_2 on Europa and Callisto. Astron J 124:3400-3403

Spencer JR, Calvin WM, Person MJ (1995) Charge-coupled-device spectra of the Galilean satellites: Molecular-oxygen on Ganymede. J Geophys Res 100:19049-19056

Spencer JR, Jessup KL, McGrath MA, Ballester GE, Yelle R (2000) Discovery of gaseous S_2 in Io's Pele plume. Science 288:1208-1210

Stansberry JA, Pisano DJ, Yelle RV (1996) The emissivity of volatile ices on Triton and Pluto. Planet Space Sci 44:945-955

Sunshine JM, A'Hearn MF, Groussin O, Li JY, Belton MJS, Delamere WA, Kissel J, Klaasen KP, McFadden LA, Meech KJ, Melosh HJ, Schultz PH, Thomas PC, Veverka J, Yeomans DK, Busko IC, Desnoyer M, Farnham TL, Feaga LM, Hampton DL, Lindler DJ, Lisse CM, Wellnitz DD (2006) Exposed water ice deposits on the surface of comet 9P/Tempel 1. Science 311:1453-1455, doi: 10.1126/science.1123632

Sunshine JM, Feaga L, Groussin O, Protopapa S, A'Hearn MF, Farnham TL, Besse S (2012) The distribution of water ice on comet 103P/Hartley 2. Asteroids, Comets, Meteors. Nigata, Japan

Sunshine JS, Farnham TL, Feaga LM, Groussin O, Merlin F, Milliken RE, A'Hearn MF (2009) Temporal and spatial variability of Lunar hydration as observed by the Deep Impact Spacecraft. Science 326:565-568, doi: 10.1126/science.1179788

Swayze GA, Clark RN, Goetz FH, Chrien TG, Gorelick NS, (2003) Effects of spectrometer band pass, sampling, and signal-to-noise ratio on spectral identification using the Tetracorder algorithm. J Geophys Res 108(E9):5105, doi: 10.1029/2002JE001975

Swayze, GA, Ehlmann, BL, Milliken, RE, Poulet, F, Wray, JJ, Rye, RO, Clark, RN, Desborough, GA, Crowley, JK, Gondet, B, Mustard, JF, Seelos, KD, Murchie, SL, and the MRO CRISM team (2008) Discovery of the acid-sulfate mineral alunite in Terra Sirenum, Mars, using MRO CRISM: possible evidence for acid-saline lacustrine deposits? Eos Trans. AGU 89(53), Fall Meet. Suppl. Abstract P44A-04

Swayze GA, Milliken RE, Clark RN, Bishop JL, Ehlmann BL, Pelkey SM, Mustard JF, Murchie SL, Brown AJ, and the MRO CRISM Team (2007) Spectral evidence for hydrated volcanic and/or impact glass on Mars with MRO CRISM. Seventh International Conference on Mars, July 9-13, 2007, Pasadena, California, LPI Contribution No. 1353, 3p

Swayze GA, Smith KS, Clark RN, Sutley SJ, Pearson RN, Rust GS, Vance JS, Hageman PL, Briggs PH, Meier AL, Singleton MJ, Roth S (2000) Using imaging spectroscopy to map acidic mine waste. Environ Sci Technol 34:47-54

Teanby NA, Irwin PGJ, de Kok R, Jolly A, Bezard B, Nixon CA, Calcutt SB (2009) Titan's stratospheric C_2N_2, C_3H_4, and C_4H_2 abundances from Cassini/CIRS far-infrared spectra. Icarus 202:620-631

Tegler SC, Cornelison DM, Grundy WM, Romanishin W, Abernathy MR, Bovyn MJ, Burt JA, Evans DE, Maleszewski CK, Thompson Z, Vilas F (2010) Methane and nitrogen abundances on Pluto and Eris. Astrophys J 725:1296-1305

Thollot P, Mangold N, Ansan V, Le Mouelic S, Milliken RE, Bishop JL, Weitz CM, Roach LH, Mustard JF, Murchie SL (2012) Most Mars minerals in a nutshell: Various alteration phases formed in a single environment in Noctis Labyrithus. J Geophys Res Planets 117:E11, doi: 10.1029/2011JE004028

Thomson BJ, Bridges NT, Milliken R, Baldridge A, Hook SJ, Crowley JK, Marion GM, de Souza Filho CR, Brown AJ, Weitz CM (2011) Constraints on the origin and evolution of the layered mound in Gale Crater, Mars using Mars Reconnaissance Orbiter data. Icarus 214:413-432

Titov DV, Svedhem H, Taylor FW, Barabash S, Bertaux JL, Drossart P, Formisano V, Häusler B, Korablev O, Markiewicz WJ, Nevejans D, Pätzold M, Piccioni G, Sauvaud JA, Zhang TL, Witasse O, Gerard JC, Fedorov A, Sanchez-Lavega A, Helbert J, Hoofs R (2009) Venus Express: Highlights of the Nominal Mission. Solar System Res 43:185-209

Tomasko MG, Archinal B, Becker T, Bezard B, Bushroe M, Combes M, Cook D, Coustenis A, de Bergh C, Dafoe L, Doose L, Doute S, Eibl A, Engel S, Gliem F, Grieger B, Holso K, Howington-Kraus E, Karkoschka E, Keller HU, Kirk R, Kramm R, Kuppers M, Lanagan P, Lellouch E, Lemmon M, Lunine J, McFarlane E, Moores J, Prout GM, Rizk B, Rosiek M, Rueffer P, Schroder SE, Schmitt B, See C, Smith P, Soderblom L, Thomas N, West R (2005) Rain, wind and haze during the Huygens probe's descent to Titan's surface. Nature 438:765-778

Trujillo CA, Brown ME, Barkume KM, Schaller EL, Rabinowitz DL (2007) The surface of 2003 EL61 in the near-infrared. Astrophys J 655:1172-1178

Tryka KA, Brown RH, Anicich V, Cruikshank DP, and Owen TC (1993) Spectroscopic determination of the phase composition and temperature of nitrogen ice on Triton. Science 261:751-754

Tryka KA, Brown RH, Anicich V, Cruikshank DP, and Owen TC, Geballe TR, and de Bergh C (1994) Temperature of nitrogen ice on Pluto and its implications for flux measurements. Icarus 112:513-527

Ustin SL, Gitelson AA, Jacquemoud S, Schaepman M, Asner GP, Gamon JA, Zarco-Tejada P (2009) Retrieval of foliar information about plant pigment systems from high resolution spectroscopy. Remote Sens Environ 113:S67–S77, doi: 10.1016/j.rse.2008.10.019

Vilas F, Domingue DL, Sprague AL, Izenberg NR, Klima RL, Jensen EA, Helbert J, D'Amore M, Stockstill-Cahill KR, Solomon SC (2012) Search for absorption features. *In:* Mercury's Visible Reflectance Spectra: Recent Results From Messenger. 43rd Lunar and Planetary Science Conference, 1330. *http://www.lpi.usra.edu/meetings/lpsc2012/pdf/1330.pdf*

Vilas F, Larson SM, Stockstill KR, Gaffey J (1996) Unraveling the zebra: Clues to the Iapetus dark material composition. Icarus 124:262-267

Vuitton V, Yelle RV, Cui J (2008) Formation and distribution of benzene on Titan. J Geophys Res 113:E05007, doi: 10.1029/2007JE002997

Wade LG (2005) Organic Chemistry, 5th edition. Prentice Hall, Inc., New Jersey

Waite H, Young D, Cravens T, Coates A, Crary F, Magee B, Westlake J (2007) The Process of Tholin Formation in Titan's Upper Atmosphere, Science 316:870-875

Wong MC, Johnson RE (1996) A three-dimensional azimuthally symmetric model atmosphere for Io .2. Plasma effect on the surface. J Geophys Res 101:23255-23259

Wray JJ, Milliken RE, Dundas CM, Swayze GA, Andrews-Hanna JC, Baldridge AM, Chojnacki M, Clark RN, Murchie SL, Ehlmann BL, Bishop JL, Seelos FP, Tornabene LL, and Squyers S (2011) Columbus crater and other possible groundwater-fed paleolakes of Terra Sirenum, Mars. J Geophys Res 116:E01001. doi: 10.1029/2010JE003694

Wyatt MB, McSween HY (2002) Spectral evidence for weathered basalt as an alternative to andesite in the northern lowlands of Mars. Nature 417:6886:263-266

Yung YL, DeMore WB (1999) Photochemistry of Planetary Atmospheres. Oxford University Press, p 201-234

Zahnle K, Schenk P, Levison H, Dones L (2003) Cratering rates in the outer solar system. Icarus 163:263-289

Zellner B (1972) On the nature of Iapetus. Astrophys J Lett 174:L107-L109

Zolotov MY, Fegley B (1998) Volcanic production of sulfur monoxide (SO) on Io. Icarus 132:431-434

Zolotov MY, Fegley B (1999) Oxidation state of volcanic gases and the interior of Io. Icarus 141:40-52

Zolotov MY, Fegley B (2000) Eruption condition of Pele volcano on Io inferred from chemistry of its volcanic plume. Geophys Res Lett 27:2789-2792